Biochimica et Biophysica Acta 1842 (2014) 1472–1484

Contents lists available at ScienceDirect

Biochimica et Biophysica Acta

journal homepage: www.elsevier.com/locate/bbadis

Mahogunin ring finger 1 suppresses misfolded polyglutamine aggregation and cytotoxicity

Deepak Chhangani [a], Nobuyuki Nukina [b,c], Masaru Kurosawa [b], Ayeman Amanullah [a], Vibhuti Joshi [a], Arun Upadhyay [a], Amit Mishra [a,*]

[a] Cellular and Molecular Neurobiology Unit, Indian Institute of Technology Jodhpur, Rajasthan 342011, India
[b] Laboratory for Structural Neuropathology, RIKEN Brain Science Institute, 2-1 Hirosawa, Wako-shi, Saitama 351-0198, Japan
[c] Department of Neuroscience for Neurodegenerative Disorders, Juntendo University Graduate School of Medicine, Tokyo 113-8421, Japan

ARTICLE INFO

Article history:
Received 20 January 2014
Received in revised form 4 April 2014
Accepted 13 April 2014
Available online 24 April 2014

Keywords:
MGRN1
Cytotoxicity
Aggregation
Polyglutamine disease

ABSTRACT

Polyglutamine diseases are a family of inherited neurodegenerative diseases caused by the expansion of CAG repeats within the coding region of target genes. Still the mechanism(s) by which polyglutamine proteins are ubiquitinated and degraded remains obscure. Here, for the first time, we demonstrate that Mahogunin 21 ring finger 1 E3 ubiquitin protein ligase is depleted in cells that express expanded-polyglutamine proteins. MGRN1 co-immunoprecipitates with expanded-polyglutamine huntingtin and ataxin-3 proteins. Furthermore, we show that MGRN1 is predominantly colocalized and recruits with polyglutamine aggregates in both cellular and transgenic mouse models. Finally, we demonstrate that the partial depletion of MGRN1 increases the rate of aggregate formation and cell death, whereas the overexpression of MGRN1 reduces the frequency of aggregate formation and provides cytoprotection against polyglutamine-induced proteotoxicity. These observations suggest that stimulating the activity of MGRN1 ubiquitin ligase might be a potential therapeutic target to eliminate the cytotoxic threat in polyglutamine diseases.

1. Introduction

A striking clinical hallmark of many neurodegenerative diseases is the presence of ubiquitin-positive intracellular inclusions formed by the aggregation of non-native neurotoxic proteins [1–3]. Numerous neurodegenerative diseases are caused by trinucleotide repeats, and polyglutamine diseases are caused by a $(CAG)_n$ expansion within the coding region of the responsible gene. Polyglutamine diseases such as Huntington's disease (HD), spinocerebellar ataxias (types 1, 2, 3, 6, 7 and 17) and X-linked spinal bulbar muscular atrophy (SBMA) are most likely caused by the neuronal dysfunction or neuronal cell death that results as the lengths of the glutamine stretches/repeats increase; early disease onset and the accumulation of intracellular aggregates are strongly linked with increased polyglutamine tract length [4–6].

The question of whether the molecular pathology that underlies polyglutamine disease is caused by a gain or a loss of function is controversial. However, the formation of intraneuronal aggregates and the deposition of inclusion bodies represent a failure of the cellular protein quality control mechanism (QC). Currently, there are no known treatments that effectively prevent or eliminate aggregate formation in polyglutamine diseases. The ubiquitin proteasome system and the autophagy pathway are two molecular mechanisms responsible for eliminating misfolded or damaged proteins in the cell, and the failure of both of these mechanisms leads to neurodegeneration [7,8]. Existing studies suggest that various chaperones, E3 ubiquitin ligases and other components of the proteasomal and autophagy degradation pathways are involved in the recognition and clearance of ubiquitin-positive intracellular aggregates [9–13].

Studies suggest that a massive accumulation of misfolded proteins impairs proteasome function, e.g., the accumulation of expanded polyglutamine proteins leads to altered proteasomal function [14–16]. Thus, the molecular mechanism for cell survival under the noxious conditions generated by protein misfolding and the failure of the ubiquitin proteasome system are of interest. Evidence suggests that under proteotoxic threat, another misfolded-protein-elimination pathway, full condition autophagy, maintains the proteostasis in cells [17–19]. In mammalian cells, three different forms of autophagy have been described: macroautophagy, chaperone-mediated autophagy (CMA) and microautophagy [20]. Autophagy promotes the clearance of α-

Abbreviations: AIP4, atrophin-interacting protein 4; Baf, bafilomycin; BMP, bis(monoacylglycero)phosphate; CMA, chaperone-mediated autophagy; CQ, chloroquine; HD, Huntington disease; HECT, homologous to E6-AP C-terminus; IB, inclusion bodies; Lamp2a, lysosome associated membrane protein 2a; MGRN1, mahogunin ring finger-1; MTT, 3-(4,5-dimethylthiazol-2-yl)-2,5-diphenyltetrazolium bromide; NEDD4, neural precursor cell expressed developmentally down-regulated protein 4; PrP, prion protein; PD, Parkinson's disease; TSG101, tumor susceptibility gene 101; RING, really interesting new gene; TBST, Tris-buffered saline Tween-20; QC, protein quality control

* Corresponding author.
E-mail address: amit@iitj.ac.in (A. Mishra).

http://dx.doi.org/10.1016/j.bbadis.2014.04.014
0925-4439/

synuclein, expanded polyglutamine proteins and mutant SOD1 proteins, and the loss of autophagy causes neurodegenerative disease in mice [2,21–24].

In the present work, we studied the detailed mechanism of the ubiquitination and degradation of expanded polyglutamine proteins by mahogunin ring finger-1 (MGRN1) E3 ubiquitin ligase through the autophagy pathway. The aberrant function of MGRN1 leads to late-onset spongiform neurodegeneration, and MGRN1 also interacts with cytosolic prion proteins (PrPs) that are linked with neurodegeneration [25,26]. Here, we report that MGRN1 interacts with expanded polyglutamine proteins and recruits with ubiquitin and p62-positive expanded polyglutamine protein aggregates in both cellular and R6/2 transgenic mouse models. Moreover, MGRN1 is involved in the ubiquitination of expanded polyglutamine proteins; the overexpression of MGRN1 reduces polyglutamine-mediated cytotoxicity and prevents polyglutamine protein-induced cell death.

2. Materials and methods

2.1. Materials

Bafilomycin, 2-mercaptoethanol, TRIzol reagent, 3-(4,5-dimethylthiazol-2-yl)-2,5-diphenyltetrazolium bromide (MTT), N6,2′-O-dibutyryladenosine-3′,5′-cyclic monophosphate (dbcAMP) and all cell culture reagents were obtained from Sigma. Lipofectamine 2000, optiMEM, plasmid pcDNA™ 3.1, ProLong® Gold Antifade Reagent, reverse transcription-polymerase chain reaction (RT-PCR) kits, Zenon®Alexa Fluor® 350 Mouse IgG1 labeling kits and Zenon®Alexa Fluor® 350 Rabbit IgG labeling kits were obtained from Life Technologies and Molecular Probes. Mouse monoclonal green fluorescent protein (GFP) antibody, nitroblue tetrazolium salt (NBT), BCIP (5-bromo-4-chloro-3-indolyl phosphate, toluidinium salt) and protein G-agarose beads were obtained from Roche Applied Science. iQ SYBR green super mix was from BioRad. Horseradish peroxidase-conjugated anti-rabbit, anti-goat and anti-mouse IgG was purchased from Amersham Biosciences. Alkaline phosphatase-conjugated anti-goat, anti-rabbit and anti-mouse IgG was purchased from Vector Laboratories. Anti-mouse IgG-fluorescein isothiocyanate and IgG-rhodamine and anti-rabbit IgG-fluorescein isothiocyanate and IgG-rhodamine were purchased from Vector Laboratories. Monoclonal anti-ubiquitin, polyclonal anti-GFP, polyclonal anti-MGRN1 (SC-160519), and monoclonal anti-actin- and MGRN1-specific siRNA oligonucleotides were purchased from Santa Cruz Biotechnology. Polyclonal anti-MGRN1 (SAB2101478) and monoclonal-anti-p62/SQSTM1 were purchased from Sigma. Rabbit polyclonal anti-ubiquitin was purchased from Dako. pEGFP-Hsp70 (Addgene-15215), plasmid pcDNA3-EGFP (Addgene 13031), pcDNA3-cmyc (Addgene 16011), pEGFP-C1-Ataxin3Q28 (Addgene-22122) and pEGFP-C1-Ataxin3Q84 (Addgene-22123) were purchased from Addgene.

2.2. Cell culture, transfection and cell viability assay

Cos-7, A549 and 293T cells were maintained in DMEM (Sigma-Aldrich). All cells were supplemented with 10% heat-inactivated fetal bovine serum, 100 U/ml penicillin and 100 μg/ml streptomycin and were grown at 37 °C in 5% CO_2. For the various experiments, cells were plated into 6-well, 24-well and 96-well tissue culture plates before one day of transfection at a subconfluent density. Lipofectamine 2000 transfection reagent was used for all transfections, in combination with various expression vectors that were used according to the manufacturers' protocols. The transfection efficiency was 80%–90% in all experiments. Cell viability was determined by 3-(4,5-dimethylthiazol-2-yl)-2,5-diphenyltetrazolium bromide, as described previously [27].

2.3. Co-immunoprecipitation and immunoblotting experiment

Cos-7 cells were transiently transfected with normal (ataxin-3(Q28) and EGFP-HDQ23) and expanded polyglutamine (ataxin-3(Q28) and EGFP-HDQ74) constructs along with the MGRN1 plasmid. After 24 h, the cells were washed with PBS and lysed on ice for 30 min with NP-40 lysis buffer (50 mM Tris, pH 8.0, 150 mM NaCl, 1% NP-40 and complete protease inhibitor cocktail). The cell lysates were prepared for immunoprecipitation by briefly sonicating before centrifugation for 15 min at 15,000 ×*g* at 4 °C. For each immunoprecipitation experiment, approximately 200 μg of protein in 0.2 ml of NP40 lysis buffer was incubated with 5 μg of primary antibody. The total cell lysate of the immunoprecipitated samples was separated by SDS-polyacrylamide gel electrophoresis and processed for immunoblotting as described elsewhere [28,29]. All primary antibodies were used at a 1:1000 dilution for immunoblotting except for GFP, which was used at a 1:2000 dilution.

2.4. Immunofluorescence techniques

Cos-7 cells were grown in two-well chamber slides and were transiently transfected with the appropriate plasmids. After transfection for 48 h, the cells were washed twice with phosphate-buffered saline, fixed with 4% paraformaldehyde in phosphate-buffered saline for 30 min, permeabilized with 0.5% Triton X-100 in phosphate-buffered saline for 5 min, washed extensively and then blocked with 5% nonfat skim milk in Tris-buffered saline-Tween 20 (TBST) [50 mM Tris, pH 7.5, 0.15 M NaCl, 0.05% Tween 20] for 1 h. In some triple-labeling experiments, primary antibodies of p62 and ubiquitin were incubated with Zenon®Alexa Fluor® kits according to the manufacturer's protocol. Primary antibody incubation was carried out overnight at 4 °C. After incubation, the cells were washed several times with TBST, incubated with rhodamine-conjugated secondary antibody (1:500 dilution) for 1 h, washed several times and finally processed for mounting as described previously [30]. Mounted slides were observed using a fluorescence microscope, and digital images were assembled using Adobe Photoshop.

2.5. Immunofluorescence staining in R6/2 mouse model of HD

For immunofluorescence staining of MGRN1, ubiquitin and p62 in the control and transgenic mouse brain sections, paraffin-embedded sections from various brain regions were deparaffinized, subjected to antigen retrieval and then processed for staining as described previously [27,31]. Appropriate FITC- and rhodamine-conjugated secondary antibodies were used to visualize expression, and all sections were mounted in ProLong® Gold Antifade Reagent (Life Technologies) before analysis of expression and colocalization. In each experiment, we used 12-week-old male R6/2 transgenic mice and control male littermates of same age; the CAG repeat sizes in the R6/2 transgenic mice were 134 CAGQ and 130Q. CAG repeat length of htt for each mouse was routinely determined by the almost same method described previously [32] to exclude the deviated repeat samples due to the instability of CAG repeat. PCR was performed with FAM-labeled primer 31329 (ATGAAGGCCTTC GAGTCCCTCAAGTCCTTC) and primer 33934 (GGCG GCTGAG GAAGCTGAGGA) followed by capillary electrophoresis with ABI 3130xl (Applied Biosystems) and analysis with Genescan software (Applied Biosystems). In immunofluorescence staining experiments we used 5 μm thick paraffin-embedded brain sections. All experiments involving mice were approved by the Animal Experiment Committee of the RIKEN Brain Science Institute.

2.6. Degradation assay, aggregate counting and statistical analysis

Cos-7 cells were plated in a 6-well tissue-cultured plate. After 24 h, the cells were transiently transfected with plasmids for the expanded

polyglutamine proteins, with or without the MGRN1 plasmid. Forty-eight hours after transfection, the cells were chased with 15 μg/ml of cycloheximide for the different time periods indicated. Cells were collected at each time point, and samples were processed for immunoblotting using the GFP antibody. Expanded polyglutamine aggregate formation was observed and counted under a fluorescence microscope (~400 transfected cells in each case). Cells retaining more than one aggregate were considered to have a single big inclusion. Statistical difference values are presented as mean ± SD. Statistical analysis between groups and intergroup comparisons were performed by using the Student's *t* test, and $p < 0.05$ indicated statistical significance. The cell viability was determined by the MTT assay as described previously [33].

2.7. Reverse transcriptase (RT) PCR analysis, quantitative real time RT-PCR analysis and RNA interference (RNAi) experiments

Cells were transfected with normal and expanded polyglutamine plasmids and we achieved about 80%–90% transfection efficiency. After 48 h of transfection, most of the expanded polyglutamine transfected cells were positive for aggregate formation and same cells were used for total RNA isolation with TRIzol reagent. Then semi-quantitative RT-PCR was carried out with an RT-PCR kit (Life Technologies). The RT-PCR analysis conditions were the same for both MGRN1 and β-actin: 30 min at 50 °C for reverse transcription of RNA, an initial denaturation step at 94 °C for 5 min and further cycling through 94 °C for 30 s denaturation, 55 °C for 45 s annealing, 72 °C for 1 min, a final extension step at 72 °C for 5 min and 5 min at 4 °C to cool down the reaction. The cycle numbers were 34 for MGRN1 and 23 for β-actin. The sequences of the various primers were as follows: MGRN1F, 5′-ATGG GCTCCATTCTCAGC-3′; MGRN1R, 5′-GTTGCTGTTGTCGCTGTTCT-3′; ActinF, 5′-TGACGGGGTCACCCACACTGTGCCCATCTA-3′; and ActinR, 5′-CTAGAAGCATTTGCGGTGGACGATGGAGGG-3′. The quantitative real time PCR for MGRN1 was performed by using iQ SYBR green super mix (BioRad) after cDNA synthesis from total RNA isolated from culture cells using TRIzol reagent. Reactions were normalized with 18S RNA as internal control and all reactions were carried out in triplicate with negative controls lacking the template DNA. The real time PCRs were done using an iCycler iQ real-time Thermocycler Detection System (Bio-Rad). MISSION® siRNA Universal Negative Control #1 (SIC001) was purchased from Sigma. MGRN1 siRNA (h): sc-92983 was obtained from Santa Cruz Biotechnology. Another set of MGRN1 predesigned siRNA was purchased from Sigma, sequence of MGRN1-siRNA (GGAUGACG AGCUGAACUUU; AAAGUUCAGCUCGUCAUCC). For RNAi experiments, EGFP-HDQ74-expressing cells were transiently transfected with either MGRN1-siRNA or Control-siRNA oligonucleotides according to the manufacturer's protocol. At various time intervals, as indicated, cell aggregate formation was counted under a fluorescence microscope. Some cells were collected and processed for RT-PCR and immunoblotting analysis. For the cell death assay, EGFP-HDQ74-expressing cells were transfected with MGRN1-siRNA or Control-siRNA oligonucleotides, and cell viability was measured by MTT assay.

3. Results

3.1. Misfolded and ubiquitinated expanded polyglutamine proteins dysregulated MGRN1 expression

Protein misfolding promotes the ubiquitination and degradation of expanded polyglutamine proteins; failure to clear these aggregated polyglutamine proteins causes neurodegenerative diseases (also referred to as polyglutamine diseases). To examine the effect of polyglutamine on endogenous MGRN1 levels, we transfected normal (ataxin-3(28Q) and EGFP-HDQ23-EGFP-tagged huntingtin exon 1 protein with 23 polyQ repeats) and expanded polyglutamine (ataxin-3(84Q) and EGFP-HDQ74-EGFP-tagged huntingtin exon 1 protein with 74 polyQ repeats) into A549 cells, as described elsewhere [34,35]. These cells form aggregates when they express polyglutamine proteins with expanded repeat lengths. We isolated total RNA from GFP-positive aggregated cells and performed RT-PCR analysis for MGRN1. To our surprise, a significant decrease in MGRN1 mRNA levels in the expanded polyglutamine ataxin-3(84Q) (Fig. 1A and C) and EGFP-HDQ74 (Fig. 1B and D) expressing cells was observed. We have noticed approximately a 0.5-fold decrease in MGRN1 mRNA levels in the expanded polyglutamine expressing cells as compared with control cells (Fig. 1E). Approximately 50–60% of cells were positive for aggregates (Fig. 1F and G) and expressed normal or expanded polyglutamine proteins (Fig. 1H and I) 48 h after transfection. Next we tested the endogenous levels of MGRN1 in normal and expanded polyglutamine expressing cells (Fig. 1J). It is surprising to notice dysregulation in MGRN1 protein levels. We speculate that this is most likely due to sequestration of endogenous MGRN1 with expanded polyglutamine proteins. To confirm this hypothesis we performed filter trap assay with cell lysates obtained from expanded polyglutamine expressing cells. As expected, we observed major association of MGRN1 protein with insoluble aggregates of expanded polyglutamine proteins (Fig. 1K). Based on the data shown in Fig. 1, we hypothesized that aggregation of expanded polyglutamine proteins promotes their sequestration and that these events might compromise MGRN1 protein function in the expanded polyglutamine-expressing cells. To test this hypothesis, we overexpressed normal and expanded polyglutamine proteins in cells and performed immunoblotting analysis using a ubiquitin antibody. As shown in Fig. 2A and B, approximately >50% of the EGFP-HDQ74 and ataxin-3(84Q)-expressing cells formed GFP-positive aggregates, and the huntingtin proteins with 74Q repeats and the ataxin-3 proteins with 84Q repeats were ubiquitinated, whereas the proteins with normal glutamine repeats did not exhibit ubiquitination. To confirm our hypothesis, we used the same samples for an immunoblotting analysis of MGRN1. We further analyzed dysregulation in the endogenous levels of MGRN1 protein in cells that expressed ubiquitinated expanded polyglutamine proteins compared with the cells that expressed non-ubiquitinated proteins with normal numbers of glutamine repeats (Fig. 2A and C).

3.2. MGRN1 interacts with the N-terminal of truncated misfolded huntingtin and ataxin-3 with expanded polyglutamine tracts

Our preliminary results suggested that MGRN1 interacts with the mutant expanded polyglutamine proteins and that this may be one of the factors involved in the dysregulation of endogenous MGRN1. We speculated that a stochastic interaction between MGRN1 and expanded polyglutamine proteins likely leads to a huge depletion of MGRN1 at the site of localization or function. To confirm this assumption, we checked the interaction of MGRN1 with expanded polyglutamine proteins. First, we overexpressed normal (ataxin-3(28Q) and EGFP-HDQ23) or expanded polyglutamine (ataxin-3(84Q) and EGFP-HDQ74) constructs in cells. Same set of cells was co-transfected with the MGRN1 construct as shown in Fig. 2D. MGRN1 was strongly and specifically immunoprecipitated with the huntingtin (EGFP-HDQ74) and ataxin-3(84Q) compared with the huntingtin (EGFP-HDQ23) and ataxin-3(28Q). Fig. 2E shows the same samples as in Fig. 2D respectively, probed with anti-GFP. We performed a detailed immunoprecipitation study using different control experiments to confirm the strong interaction of MGRN1 with the N-terminals of expanded polyglutamine huntingtin and ataxin-3 proteins. We further transfected normal and expanded polyglutamine constructs of the N-terminals of huntingtin or ataxin-3 proteins. Cell lysates were immunoprecipitated with beads only (control) (Fig. 2F) and normal IgG (Fig. 2G and H), and the blots were probed with anti-MGRN1 and anti-GFP antibodies as indicated in Fig. 2F, G and H. To further confirm the interaction of MGRN1 and expanded polyglutamine proteins, we pulled the cell lysates with MGRN1 antibody and blots were processed with anti-GFP (Fig. 2I) and for the control experiment only the GFP expressed cell lysates were used to

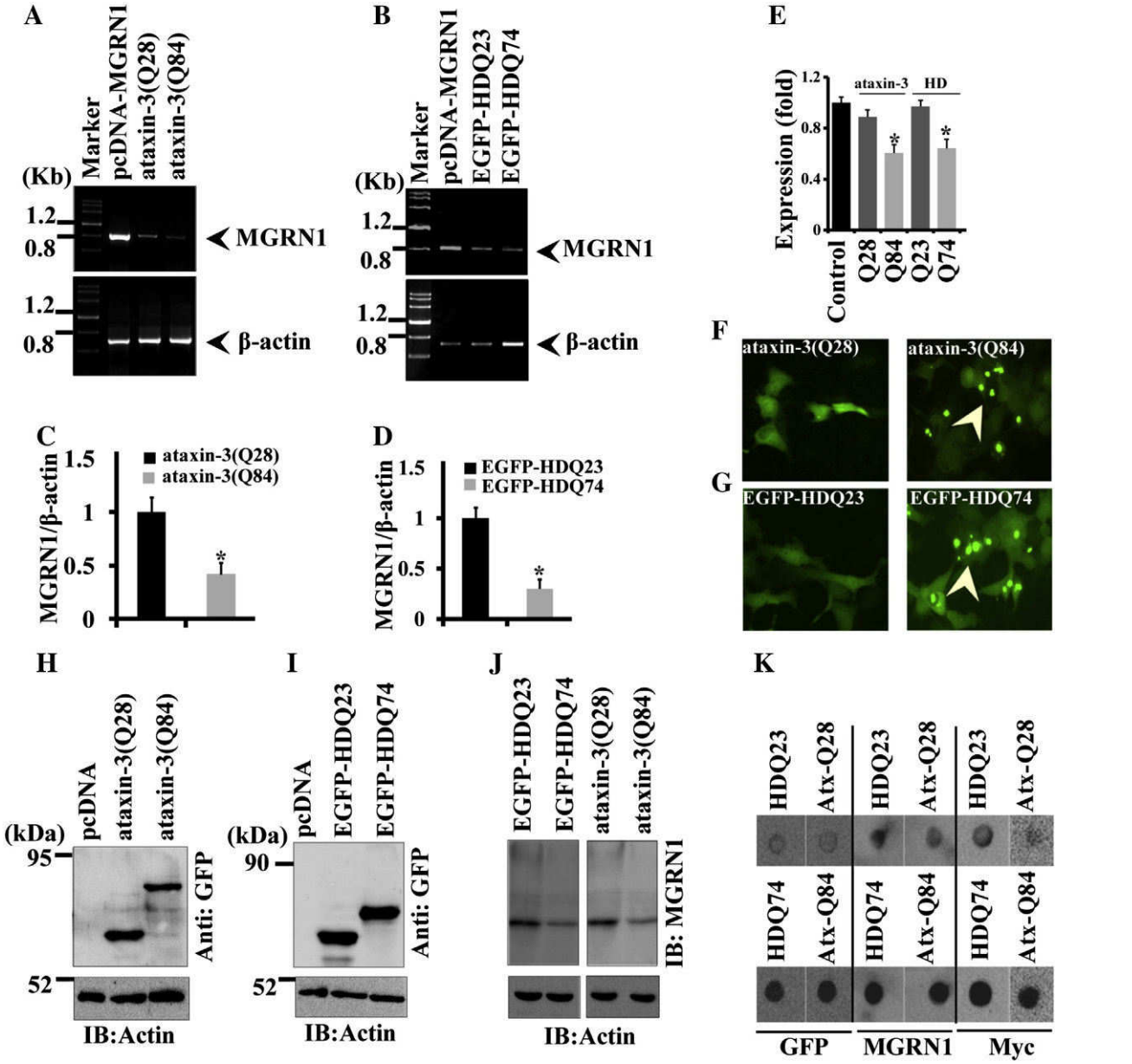

Fig. 1. MGRN1 dysregulation in expanded polyglutamine-expressing cells. (A–B) A549 cells were transfected with ataxin-3 (A) or EGFP-HD (B) normal and polyglutamine-expanded expression plasmids as indicated. After 48 h, total RNA was isolated from the cells and processed for RT-PCR analysis using MGRN1 and β-actin primers. (C–D) The bar diagram represents the quantitation of the MGRN1 band intensities shown in A and B. Data were collected from three independent experiments using NIH image analysis software and normalized to the levels of β-actin. Values are the mean ± SD. *, $p < 0.05$ compared with ataxin-3(Q28)- (C) and EGFP-HDQ23- (D) expressing cells. (E) Cells were transiently ataxin or EGFP-HD normal and polyglutamine-expanded expression plasmids including control (pcDNA) plasmid. After 48 h, quantitation of MGRN1 mRNA levels using quantitative real time RT-PCR in the experiment. (F–G) Aggregate formation in ataxin-3(Q84)- (F) and EGFP-HDQ74- (G) expressing cells. (H–I) The same cells were subjected to immunoblotting analysis using GFP and actin antibodies. (J–K) Cells were co-transfected as described above with ataxin-3-GFP fusion normal (ataxin-3(Q28)) and expanded polyglutamine (ataxin-3(Q84)) and EGFP-HD (normal (EGFP-HDQ23) and polyglutamine-expanded (EGFP-HDQ74)) constructs. Forty-eight hours after transfection, the cells were collected and processed for immunoblotting with MGRN1and actin antibodies (J). Some cells were cotransfected Myc-MGRN1 plasmid. Same cell lysates were processed for filter-trap analysis by probing with anti-GFP, anti-MGRN1 and anti-Myc antibodies (K).

immunoprecipitate with the MGRN1 antibody and blot was detected with the GFP antibody (Fig. 2J). These results confirmed our finding that MGRN1 strongly interacts with the N-terminals of huntingtin and ataxin-3 proteins with expanded polyglutamine tracts.

3.3. Association and recruitment of MGRN1 with polyglutamine aggregates

To examine whether the subcellular localization of endogenous MGRN1 is affected by polyglutamine aggregates, we transfected normal and expanded polyglutamine protein huntingtin (EGFP-HDQ23 (Fig. 3A) and EGFP-HDQ74) (Fig. 3B) and ataxin-3 (ataxin-3(28Q) (Fig. 3E) and ataxin-3(84Q)) (Fig. 3F) constructs in cells. After transfection, cells were subjected to immunofluorescence staining using MGRN1 antibody. Endogenous MGRN1 was recruited with the huntingtin and ataxin-3 expanded polyglutamine aggregates in cells as shown in Fig. 3. Next, we further co-transfected huntingtin (EGFP-HDQ23 and EGFP-HDQ74) and ataxin-3 (ataxin-3(28Q) and ataxin-3(84Q)) constructs with the MGRN1 plasmid. After 48 h of transfection, cells were subjected to immunofluorescence experiments using the anti-MGRN1 antibody. MGRN1 was localized to the cytoplasm with partial or diffuse staining in the nucleus of cells expressing normal numbers of glutamine repeats, shown in Fig. 3C (EGFP-HDQ23), and Fig. 3G (ataxin-3(28Q)). However, MGRN1 was co-localized and associated with the aggregates of proteins with expanded polyglutamine repeats

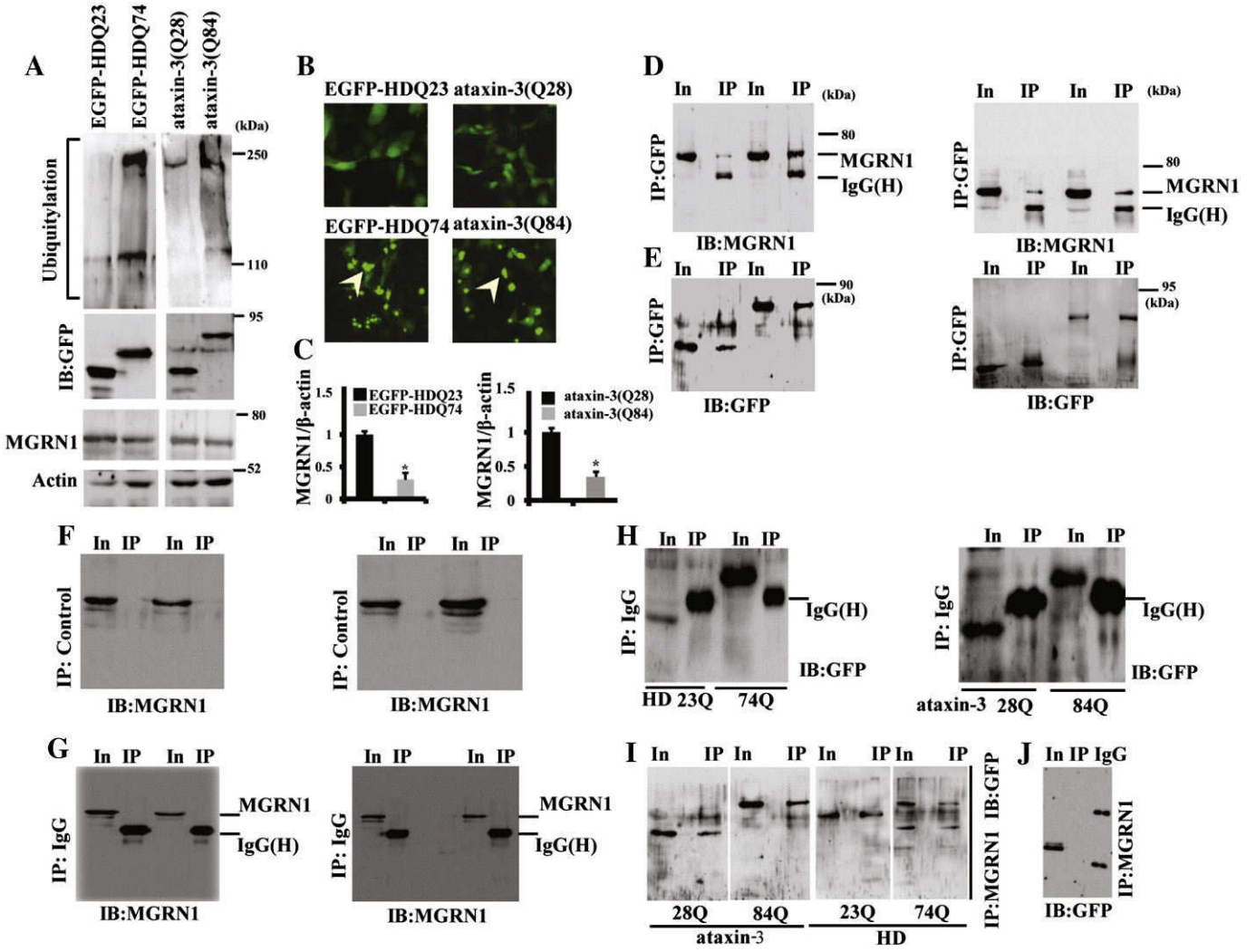

Fig. 2. Ubiquitination of expanded polyglutamine proteins depletes the endogenous level of MGRN1 protein and interaction of MGRN1 with soluble misfolded normal and expanded polyglutamine proteins. (A) Ataxin-3 normal (ataxin-3(Q28)) and expanded polyglutamine (ataxin-3(Q84)) and EGFP-HD (normal (EGFP-HDQ23) and polyglutamine-expanded (EGFP-HDQ74)) plasmids were transiently transfected in 293T cells; 48 h after transfection, the cells were subjected to immunoblotting analysis using ubiquitin, GFP, MGRN1 and actin antibodies. (B) Aggregate formation in expanded polyglutamine-expressing cells transfected with (ataxin-3(Q84) and EGFP-HDQ74) constructs. Arrows indicate the formation of aggregates in the expanded polyglutamine expressing cells. (C) Quantification of endogenous MGRN1 levels collected from three independent experiments using NIH Image analysis software. Data were normalized using actin. Values are the mean ± SD. *$p < 0.05$ with respect to cells expressing proteins with normal numbers of glutamine repeats. (D–E) Transfection was used to overexpress Myc-MGRN1 and normal (EGFP-HDQ23) and polyglutamine-expanded (EGFP-HDQ74) and ataxin-3 normal (ataxin-3(Q28)) and expanded polyglutamine (ataxin-3(Q84)) constructs in Cos-7 cells. After 48 h of transfection, the cell lysates were processed for immunoprecipitation (IP) with a GFP antibody. Blots were sequentially probed with anti-MGRN1 (D) and anti-GFP (E). (F) Cell lysates were collected from ataxin-3 and EGFP-HD normal and expanded polyglutamine-expressing cells and processed for IP by beads alone (control-IP) and blots were developed by anti-MGRN1. (G–H) As described above some cell lysates were used immunoprecipitation (IP) with normal IgG and blots were probed with anti-MGRN1 (G) and anti-GFP antibodies (H). (I) Cells were transfected with normal (EGFP-HDQ23) and polyglutamine-expanded (EGFP-HDQ74) constructs and lysates were processed for IP by anti-MGRN1 and blots were developed with anti-GFP. (J) Cells were transfected with only GFP expressing construct and lysates were processed for IP with MGRN1antibody and blot was developed with GFP antibody. Immunoprecipitants were subject to immunoblotting analysis with the indicated antibodies.

in EGFP-HDQ74- and ataxin-3(84Q)-expressing cells (Fig. 3D and H). Control experiment (without secondary antibody) for recruitments of MGRN1 with expanded polyglutamine aggregates was performed with EGFP-HDQ23 and EGFP-HDQ74 expressing cells (Supplementary Fig. S1). To further confirm that the polyglutamine aggregates are positive for MGRN1, we performed triple-immunofluorescence staining. As shown in Fig. 4A, MGRN1 was present in the cytoplasm and had a diffuse localization or staining pattern with p62 and ubiquitin in EGFP-HDQ23-expressing cells with a normal number of glutamine repeats. Strikingly, MGRN1 recruits and co-localizes with p62 and ubiquitin double-positive aggregates of expanded polyglutamine proteins (Fig. 4A and B, lower panel). These results indicate a strong and specific interaction between MGRN1 and misfolded-expanded polyglutamine proteins or their aggregates.

3.4. Recruitment and co-localization of MGRN1 with p62 and ubiquitin into neuronal aggregates of mutant huntingtin in the brains of R6/2 transgenic mice

To confirm our current finding that MGRN1 interacts and associates with p62 and ubiquitin polyglutamine aggregates in cellular models, we examined the recruitment and co-localization of MGRN1 in the R6/2 transgenic mouse brain, which models HD onset. We compared the MGRN1 localization profiles in control and R6/2 mice. Immunofluorescence staining showed that in control mice, MGRN1 was predominantly expressed in the cytoplasmic compartment of cerebellar Purkinje cells and in cortical neurons. However, in R6/2 HD transgenic mice, MGRN1 was strongly recruited to neuronal p62-positive aggregates in cerebellar Purkinje cells and in cortical neurons (Fig. 5A and B). To confirm the

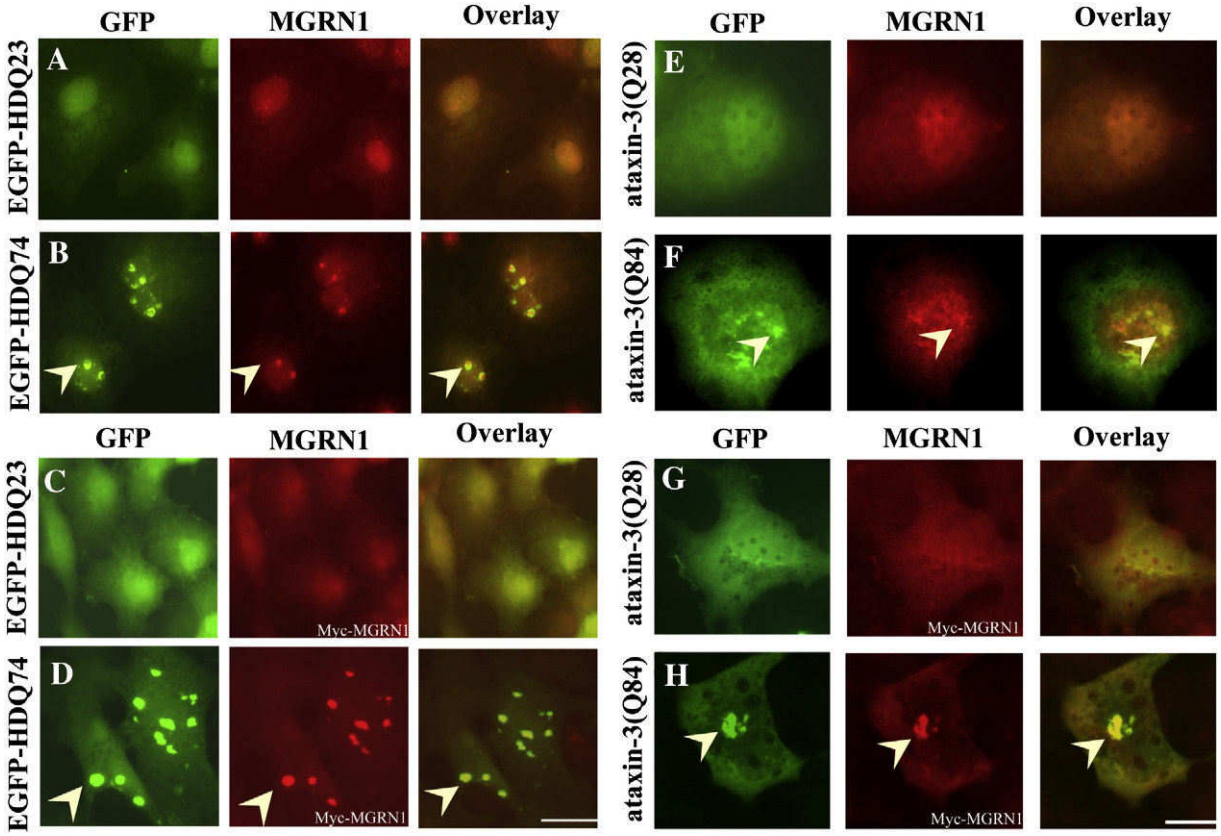

Fig. 3. MGRN1 associates with huntingtin expanded polyglutamine aggregates and recruitment of MGRN1 to ataxin-3 aggregates. (A–B) Cos-7 cells were transiently transfected with EGFP-HDQ23 (A) EGFP-HDQ74 (B) constructs and after 48 h of transfection, the cells were processed for immunofluorescence staining for MGRN1 (red) and normal and expanded polyglutamine expressions (green). (C–D) EGFP-HDQ23 (C) and EGFP-HDQ74 (D) expressing Cos-7 cells were transiently transfected with Myc-MGRN1 plasmid. Thirty-six hours after transfection, cells were subjected to immunofluorescence staining with anti-MGRN1 (red). A rhodamine-conjugated secondary antibody was used to label MGRN1. Arrows indicate the recruitment of MGRN1 to the huntingtin aggregates. (E–F) Cos-7 cells were transiently transfected with ataxin-3-GFP fusion normal (E) (ataxin-3(Q28)) and expanded (F) polyglutamine (ataxin-3(Q84)) constructs. Post transfected cells were subjected to immunofluorescence staining for MGRN1 (red) and normal and expanded polyglutamine expressions (green). (G–H) Sub-confluent Cos-7 cells were plated into 2-well chamber slides and co-transfected with ataxin-3-GFP fusion constructs containing (ataxin-3(Q28)) (G) and (ataxin-3(Q84)) (H) polyglutamine constructs along with Myc-MGRN1 plasmid as indicated. After transfection, the cells were fixed in 4% paraformaldehyde and then processed for immunofluorescence with MGRN1 antibody. MGRN1 was visualized with rhodamine-conjugated secondary antibody (red). Arrows indicate the recruitment of MGRN1 to ataxin-3 aggregates. Scale bar, 20 μm.

recruitment of MGRN1 with neuronal aggregates of mutant huntingtin in the R6/2 HD mouse model, we performed double-immunofluorescence staining studies using MGRN1 and ubiquitin antibodies. Analysis of these results showed that more than 70%–80% of the ubiquitin positive aggregates were co-localized and recruited with the MGRN1 protein in the different brain regions of the HD R6/2 transgenic mouse model (Fig. 6A and B). We further confirmed that these neuronal (NeuN) positive aggregates (Fig. 7A and B) were also positive for huntingtin staining and colocalize with MGRN1 and p62 inclusions in R6/2 transgenic mice brain (Fig. 7C and D). We further performed the quantification of same samples and observed that the normal MGRN1 bearing neurons were decreased in HD R6/2 transgenic mouse model (Fig. 7E and F).

3.5. MGRN1 promotes the ubiquitination of polyglutamine-expanded proteins

The overburden or massive production of misfolded proteins can impair the ubiquitin proteasome system [36]. To avoid such a drastic problem and to promote the clearance of toxic soluble misfolded intermediates, cells adopt another strategy, i.e., autophagy-mediated clearance [37]. In the current study, we noticed the deregulation and strong association of MGRN1 with expanded polyglutamine proteins, and therefore we posed the question: how does MGRN1 respond to expanded polyglutamine proteins and target them for elimination? We co-expressed truncated N-terminal huntingtin (EGFP-HDQ74) with wild-type MGRN1 or its catalytic inactive mutant MGRN1 (AVVA) form. As shown in Fig. 8A, we observed that the overexpression of the wild-type MGRN1 promotes the ubiquitination of EGFP-HDQ74 polyglutamine intermediates. To confirm this finding, we precipitated cell lysates from various experiments with GFP antibody, and blots were probed using an anti-ubiquitin antibody. We speculated that MGRN1 interaction with expanded polyglutamine proteins could induce their ubiquitination. To validate this assumption we processed immunoprecipitation in cells expressing expanded polyglutamine proteins using GFP antibody and blots were probed with ubiquitin antibody. Cell lysates obtained from expanded polyglutamine proteins were centrifuged at 10,000 $\times g$ at room temperature for 5 min and the separated pellet and supernatant fractions were analyzed by immunoblotting with antibodies against GFP and MGRN1. In pellet samples, higher molecular protein complex of expanded polyglutamine proteins retained in stacking gel (Fig. 8B). As shown in Fig. 8C, overexpression of wild-type MGRN1 caused a significant increase in the accumulation of ubiquitinated derivatives of EGFP-HDQ74 proteins. Bafilomycin, an autophagy inhibitor, also induces the accumulation of ubiquitinated EGFP-HDQ74 proteins (Fig. 8C, left panel). Bafilomycin treatment caused massive aggregate formation and the accumulation of high-molecular-weight complexes of the expanded polyglutamine proteins, which suggests that polyglutamine aggregation is also cleared by the autophagy pathway (Fig. 8C, upper panel). As earlier reported, MGRN1 enhances the proteasome-independent ubiquitination of tumor-susceptibility gene 101 (TSG101) [38]. ITCH is another E3 ubiquitin ligase, which induces the degradation of Deltex (DTX) via lysosomal

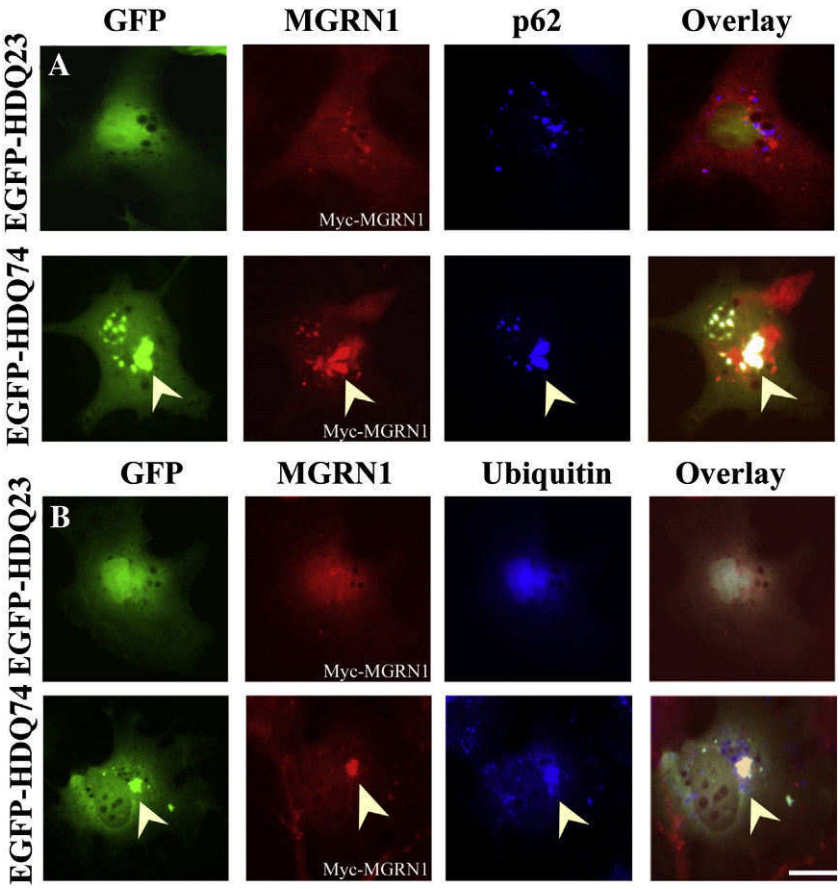

Fig. 4. MGRN1 co-localization with huntingtin expanded-polyglutamine p62 and ubiquitin-positive aggregates in cells. (A) Cos-7 cells were transiently co-transfected with EGFP-HDQ74 construct and Myc-MGRN1 plasmid. After 48 h of transfection, the cells were subjected to triple-immunofluorescence staining for MGRN1 (red), p62 (blue) and EGFP-HDQ74 expressions (green) as described in the "experimental procedure". Arrows indicate the recruitment of MGRN1 to huntingtin expanded-polyglutamine aggregates that are positive for p62 staining. Scale bar, 20 μm. (B) As described above, some cells were subjected to triple-immunofluorescence staining for MGRN1 (red), ubiquitin (blue) and EGFP-HDQ74 expressions (green). The arrows indicate the co-localization of ubiquitin-positive huntingtin expanded-polyglutamine aggregates and MGRN1. Scale bar, 20 μm.

pathway and colocalizes with endocytic vesicles [39]. Nedd4 (neuronal precursor cell-expressed, developmentally down-regulated gene 4) is a HECT-domain ubiquitin ligase, which enhances the degradation of α-synuclein by the endo-lysosomal pathway [40]. These studies also support our hypothesis that probably MGRN1 can promote the ubiquitination of expanded polyglutamine through the autophagy pathway. As shown in Fig. 8D and E, transiently transfected overexpressed wild-type MGRN1 overexpression decreases the levels of EGFP-HDQ74 expanded polyglutamine proteins, which can be prevented upon the addition of the autophagy inhibitor bafilomycin (Fig. 8F and G). Earlier it has been shown that improper sequestration of MGRN1 with cytosolic prion proteins contributes in neurodegeneration and MGRN1 interacts with Hsp70 chaperone [25,41]. Therefore it may be possible that MGRN1 targets expanded polyglutamine proteins anchored with Hsp70 chaperone and promotes their clearance from the dense cellular pool, however for better understanding in near future it needs further study in detail.

3.6. MGRN1 suppresses aggregate formation and polyglutamine-induced cell death

Because we observed that MGRN1 enhances the ubiquitination and elimination of expanded polyglutamine proteins, we wondered whether MGRN1 could affect polyglutamine protein aggregation and polyglutamine protein-induced cell death. Therefore, we co-transfected 293T cells with huntingtin (EGFP-HDQ74) and MGRN1 or MGRN1-siRNA. As shown in Fig. 9A, aggregate formation was decreased by the overexpression of MGRN1. However, the number of aggregates increased in cells transfected with MGRN1-siRNA. The overexpression of MGRN1 enhances the clearance of expanded polyglutamine proteins, and downregulation promotes the accumulation of polyglutamine proteins (Fig. 9B). The overexpression of MGRN1 significantly suppresses aggregate formation in a concentration-dependent manner (Fig. 9C). Interestingly, the suppression of aggregate formation and cytoprotective affect against ER and heat stress was more pronounced when MGRN1 was overexpressed along with Hsp70 (Fig. 9E and G). Quantitative data from cells transfected with MGRN1-siRNA in a concentration-dependent manner showed a dose-dependent increase in the rate of aggregate formation, confirming the effect of MGRN1 on polyglutamine aggregate formation (Fig. 9D). The knockdown of the endogenous levels of MGRN1 also significantly induced death in polyglutamine (74Q)-expressing cells (Fig. 9F). We further confirm the cumulative cytoprotective role of MGRN1 and Hsp70 under various stress conditions; therefore we exposed cells with ER and heat stress conditions and observed that Hsp70 overexpression alleviates cytotoxicity under different stress conditions (Fig. 9G). Taken together, our data suggest that MGRN1 reduces the formation of aggregates of expanded polyglutamine proteins and protects cells from death mediated by the proteotoxic effects of polyglutamine proteins.

4. Discussion

Cells eliminate abnormal proteins with the help of a protein quality control mechanism (QC). Expanded polyglutamine proteins induced multifactorial deleterious events in cells. Numerous E3s, such as Gp78, E6-AP, CHIP, Parkin, Hrd1 and Malin, play a crucial role in the clearance of polyglutamine proteins, reducing their aggregate formation and

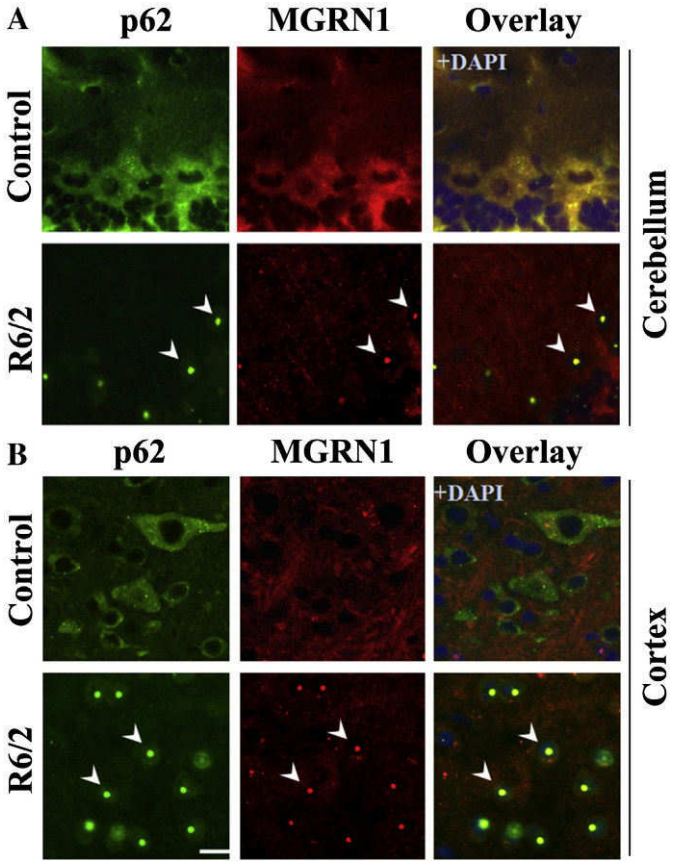

Fig. 5. Redistribution and association of MGRN1 with p62-positive aggregates in R6/2 transgenic mice. (A–B) Immunofluorescence double-labeling of MGRN1 and p62 in the brain of R6/2 mouse. Adult mouse brain sections of the cerebellum (A) and cortex (B) from control and R6/2 mice were incubated with p62 (green) and MGRN1 (red) antibodies. In the overlay (yellow) image, arrows indicate the aggregates of the expanded huntingtin that co-localize with p62 and MGRN1 with DAPI (blue) staining. Merging (yellow) illustrates co-localization of MGRN1 and p62 in the inclusions. Scale bar, 20 μm.

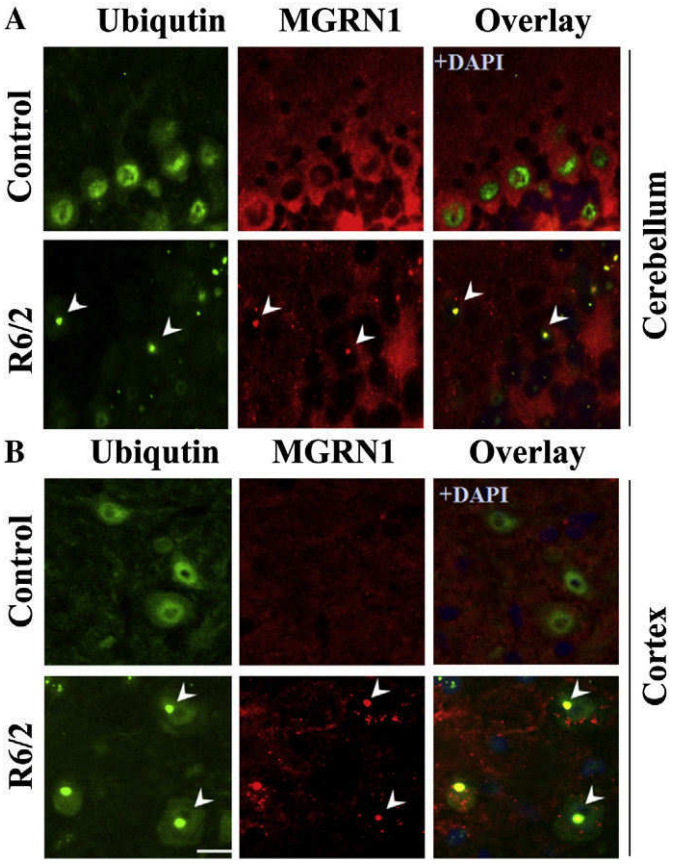

Fig. 6. Co-localization of MGRN1 with ubiquitin-positive aggregates in the neurons of the transgenic R6/2 mouse model of Huntington's disease. (A–B) Sections from the adult mouse brain subjected to immunofluorescence staining with anti-ubiquitin and anti-MGRN1 in the cerebellum (A) and cortex (B) of control and R6/2 transgenic mice. The FITC-conjugated secondary antibody was used to label the ubiquitin, and rhodamine-conjugated secondary antibody was used to stain MGRN1. Arrows indicate the aggregates of expanded huntingtin that co-localize with MGRN1 and ubiquitin. The overlay images also show DAPI staining of the cell nuclei. Scale bar, 20 μm.

alleviating poly (Q)-proteotoxicity [5,31,42–45]. Here, we identified that mahogunin ring finger-1 (MGRN1), a putative E3 ubiquitin ligase, interacts with misfolded and ubiquitinated expanded polyglutamine proteins in a cellular model of HD. Additionally, we observed the recruitment and co-localization of MGRN1 ubiquitin ligase in various brain regions in the R6/2 transgenic mouse model of HD. Finally, we showed that overexpression of MGRN1 facilitates the elimination of misfolded polyglutamine proteins via autophagy and reduces aggregate formation and cell death in expanded polyglutamine-expressing cells.

The overburden of misfolded or non-native protein aggregation impairs the function of the ubiquitin proteasome system [36,46]. However, how the accumulation or aggregation of polyglutamine proteins impairs the function of the ubiquitin proteasome system and contributes to the pathomechanism of the disease is still controversial [47–51]. Previous studies indicate that the aggregation of polyglutamine proteins significantly impairs the activity of the proteasome against stress-induced protein aggregation [27,52]. However, we do not know how cells survive the proteasome dysfunction caused by massive polyglutamine protein aggregation. Thus, it is important to understand what other cellular factors or pathways are involved in cell survival and the mechanisms that inhibit polyglutamine-mediated cellular toxicity. Reports suggest that to avoid these noxious conditions and to eliminate the misfolded protein load, the cellular protein quality control mechanism (QC) adopts another survival strategy, i.e., autophagy-mediated clearance [37,53,54]. Neural precursor cells that express both developmentally downregulated protein 4 (NEDD4) and atrophin-interacting protein 4 (AIP4)/Itch E3 ubiquitin ligases promote the clearance of melanocytic transmembrane proteins (i.e., Melan-A/MART-1) by lysosomes [55]. MGRN1 is a ring finger-1 E3 ubiquitin ligase that is involved in spongiform neurodegeneration encephalopathy. Recently it has been observed that MGRN1 overexpression and loss of function do not influence prion disease; possibly functional sequestration of MGRN1 may cause cytosolic PrP linked neurotoxicity [56]. We have shown that MGRN1 overexpression reduces the aggregation of chaperone associated misfolded proteins in cells [41]. MGRN1 facilitates the ubiquitination and degradation of tumor-susceptibility gene 101 (TSG101) via the endolysosomal pathway [57].

Earlier it has been proposed that cytosolic prion protein exposure disrupts the function of MGRN1 that contributes in neurodegeneration [25]. In our current study we have also observed that MGRN1 mRNA and protein levels were reduced in the poly (Q) expanded huntingtin- and ataxin-3 fragment-expressing cells. Why were endogenous MGRN1 levels depleted in polyglutamine-expressing cells? Previous studies elaborate that the interaction of polyglutamine aggregates interrupts the normal function of various transcription factors such as nuclear factor kappa-light-chain-enhancer of activated B cells (NF-κB), CREB binding protein (CBP), TATA box binding protein (TBP) and specificity protein 1 (Sp1) [58–62]. Most probably sequestration and depleted function of these transcriptions contribute in the molecular pathomechanism of polyglutamine diseases. Overall these studies also support our current speculation that MGRN1 interacts with polyglutamine aggregated intermediate species for their clearance. It is possible that this interaction leads to the co-aggregation and

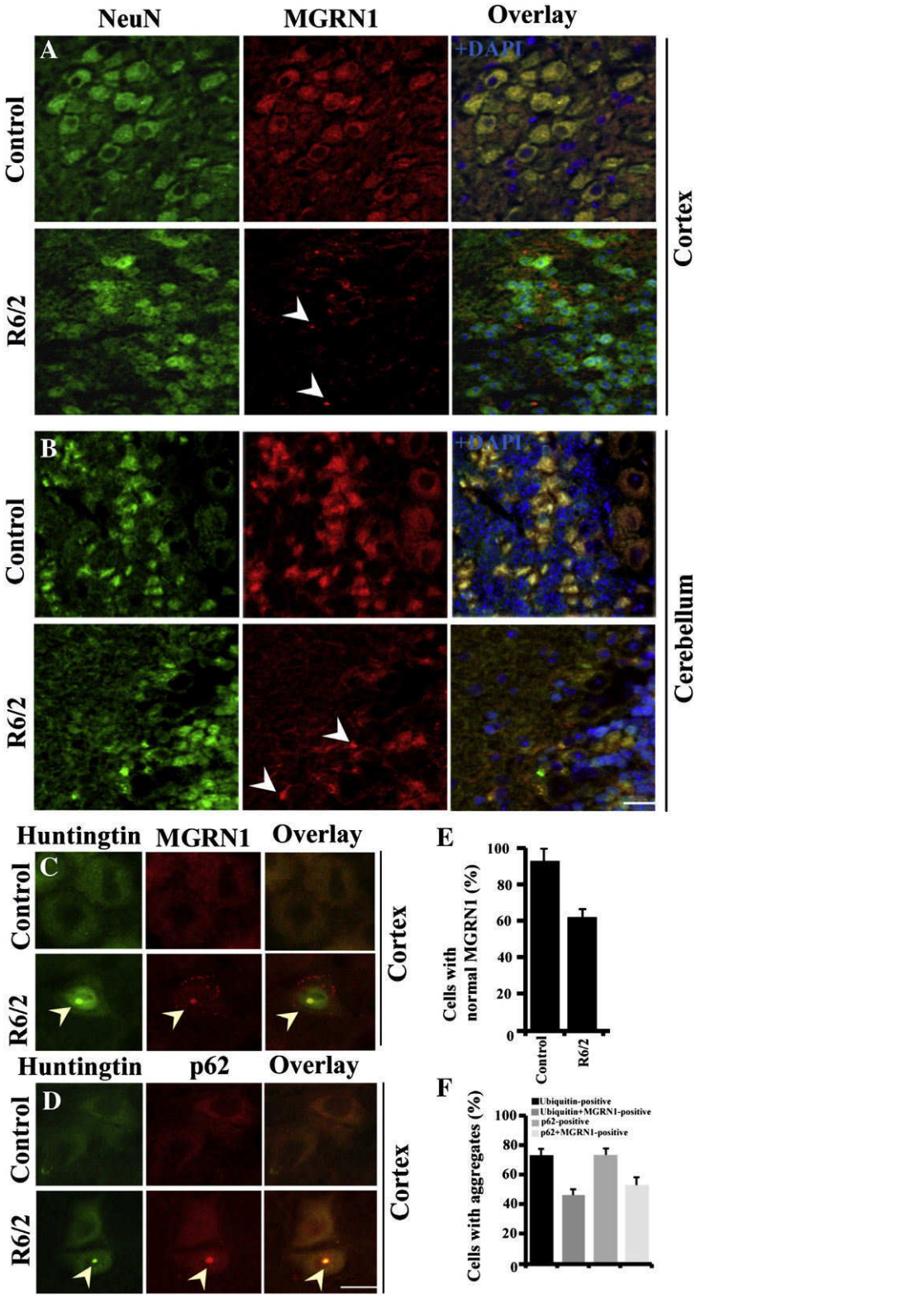

Fig. 7. Recruitment of p62 and MGRN1 with huntingtin-positive aggregates in the neurons of the transgenic R6/2 mouse model of Huntington's disease. (A–B) Brain sections of R6/2 mice were immunostained for NeuN (green) and MGRN1 (red) in cortex (A) and cerebellum (B) regions. The FITC-conjugated secondary antibody was used to label the NeuN, and rhodamine-conjugated secondary antibody was used to stain MGRN1. Arrows indicate MGRN1-positive aggregates in the neurons. (C) Sections from the adult mouse brain processed to immunofluorescence staining with anti-huntingtin and MGRN1 antibody in the control and R6/2 transgenic mice. The FITC-conjugated secondary antibody was used to label the huntingtin, and rhodamine-conjugated secondary antibody was used to stain MGRN1. Arrows indicate the aggregates of expanded huntingtin that co-localize with MGRN1. (D) Double immunofluorescence staining of p62 and huntingtin in the brain of an R6/2 mouse. Adult mouse brain sections from control and R6/2 mice were probed with huntingtin (green) and p62 (red) antibodies. In the overlay (yellow) image, arrows indicate the aggregates of the expanded huntingtin that co-localize with p62 staining. Merging (yellow) illustrates co-localization of MGRN1 and huntingtin in the inclusions. Scale bar, 20 μm. (E) Percentage of neurons with normal MGRN1 staining per total cortical neurons from B6. (F) Quantitative analysis of p62, ubiquitin and MGRN1 positive inclusions in the HD transgenic mice brain sections along with their age-matched control.

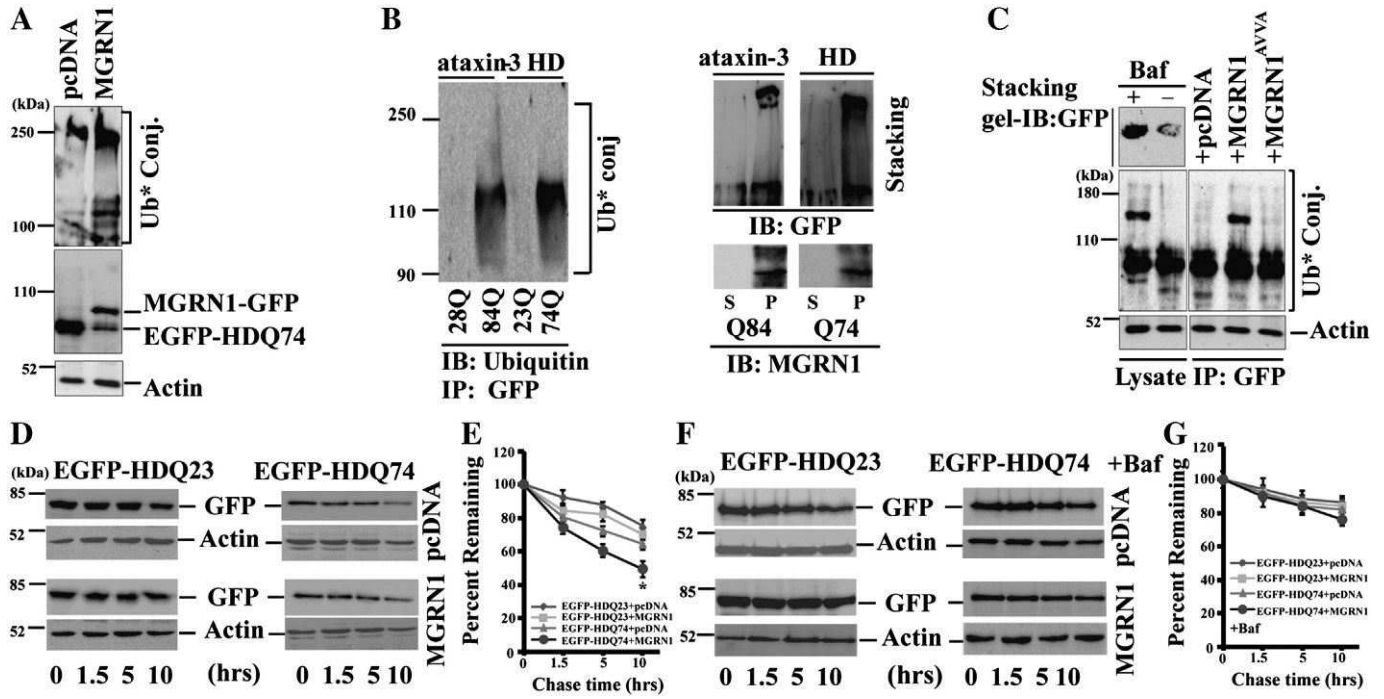

Fig. 8. MGRN1 overexpression induces the ubiquitination of polyglutamine-expanded proteins. (A) Cos-7 cells were transiently co-transfected with MGRN1-GFP and EGFP-HDQ74 constructs. After 48 h, the cells were subjected to immunoblotting analysis by using anti-ubiquitin, anti-GFP and anti-actin. (B) Cells were transfected with normal (EGFP-HDQ23) and polyglutamine-expanded (EGFP-HDQ74) constructs and lysates were processed for IP by GFP antibody and blot was developed with anti-ubiquitin. Cell lysates obtained from expanded polyglutamine proteins were separated in supernatant and pellet fractions and performed immunoblotting with anti-GFP and anti-MGRN1 antibodies (B). (C) The same cells were treated with or without 50 nM bafilomycin (Baf) for 12 h and subjected to immunoblotting analysis with GFP antibody. Some cells were co-transfected with MGRN1 (AVVA)-GFP mutant plasmid and the EGFP-HDQ74 construct. Cell lysates were subjected to immunoprecipitation (IP) using GFP antibody, and blots were probed with GFP, ubiquitin and actin antibodies. (D) Cos-7 cells were transiently co-transfected with EGFP-HDQ23 and EGFP-HDQ74 constructs with MGRN1. At 48 h after transfection, the cells were treated with cycloheximide (15 μg/ml) and chased for different periods. Blots were detected with GFP and actin antibodies. (E) Quantitation of the blot band intensities from three independent experiments was performed using NIH Image analysis software. Values are the mean ± SD. (F) As described in C plus treatment with 50 nM bafilomycin (Baf). Blots were detected with GFP and actin antibodies. (G) The line graph shows the quantitation of the blot band intensities from three independent experiments performed using NIH Image analysis software. Values are the mean ± SD. *, $p < 0.05$ compared with control.

sequestration of MGRN1 with the existing polyglutamine protein aggregates, and this prolonged mislocalization may lead to the depletion of MGRN1, most likely contributing to the pathogenesis of polyglutamine diseases. In the present study, we confirmed the interaction of MGRN1 with expanded polyglutamine proteins via a detailed co-immunoprecipitation study and observed the co-localization of MGRN1 with cellular aggregates of poly (Q) expanded huntingtin and ataxin-3 protein. Previously, malin E3 ubiquitin ligase was shown to associate with ubiquitinated Lafora bodies, and the loss of malin function most likely contributes to the pathogenesis of Lafora disease [63]. The malin E3 ubiquitin ligase study supports our current findings; to validate this novel interaction, we used triple-immunofluorescence analysis and report the co-localization of MGRN1 with p62 and ubiquitin-positive polyglutamine aggregates in cells.

Based on the interaction and co-localization of MGRN1 with expanded polyglutamine proteins in the cellular model of HD disease, we observed the recruitment of MGRN1 to the neuronal aggregates in R6/2 transgenic mice. In this mouse model of HD disease, we were able to detect a significant number of aggregates that were positive for MGRN1, p62 and ubiquitin staining and a clear redistribution of MGRN1 from the cytoplasm to the aggregates in the cerebellar Purkinje cells and cortical neurons. These results prompted us to investigate the functional role of MGRN1 in the elimination of expanded polyglutamine proteins and the consequent effect of this degradation on aggregate formation. We showed that autophagy inhibition induces the ubiquitination of expanded polyglutamine proteins. Induced autophagy retains an ability to reduce the toxicity of expanded polyglutamine proteins [64]. Our observations demonstrated that MGRN1 overexpression specifically stimulates the rate of degradation of the polyglutamine protein expansions and reduces aggregate formation, providing a cytoprotective response against polyglutamine-induced toxicity. This result was confirmed by the depletion of MGRN1 levels by siRNA, which increased the accumulation of expanded polyglutamine protein aggregates and enhanced the poly (Q) expansion-induced cell death. Interestingly, we noted that the protective response was more prominent when MGRN1 and the Hsp70 chaperone were co-expressed.

The identification of an E3 ubiquitin ligase that is capable of eliminating misfolded aggregated proteins represents a potential therapeutic approach against diseases caused by disordered proteins. There are numerous studies implicating autophagy or selective autophagy in polyglutamine diseases [65–67]. However, the detailed molecular function of autophagy in the selective recognition of expanded polyglutamine proteins is still not well understood. Our current study indicates that the recruitment of MGRN1 with expanded polyglutamine proteins occurs in cellular and mouse models of HD disease. Together, our results suggest that MGRN1 interacts with expanded polyglutamine proteins; the association of MGRN1 promotes the ubiquitination and elimination of poly (Q) expansions that eventually alleviate aggregation and cell death. MGRN1 provides cytoprotection against polyglutamine induced toxicity and probably its aberrant function plays a crucial role in the pathomechanism of neurodegeneration and possibly holds therapeutic potential for treating protein-disordered diseases.

Supplementary data to this article can be found online at http://dx.doi.org/10.1016/j.bbadis.2014.04.014.

Acknowledgement

This work was supported by the Department of Biotechnology, Government of India. AM was supported by Ramalinganswami Fellowship (BT/RLF/Re-entry/11/2010) and Innovative Young Biotechnologist

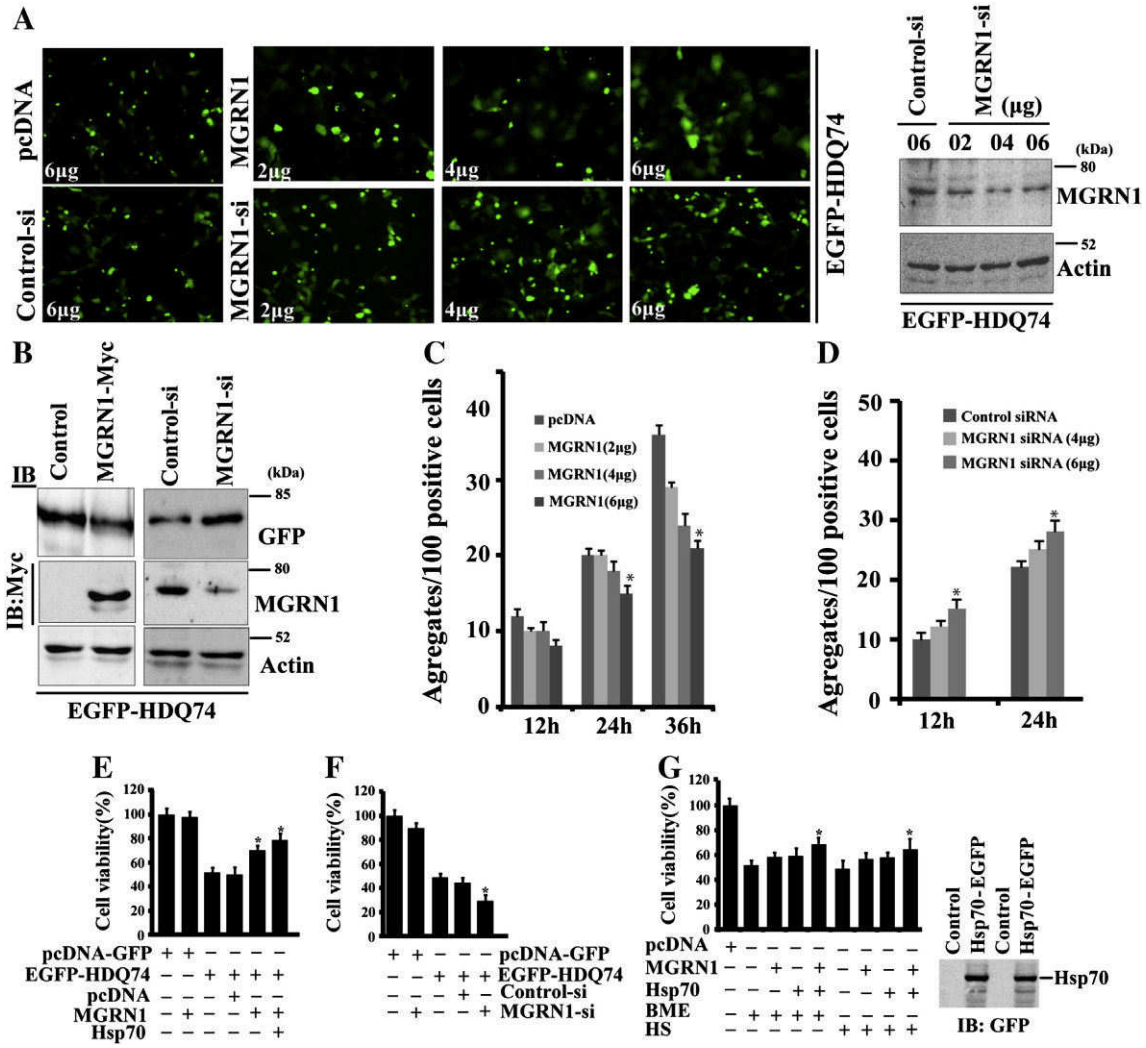

Fig. 9. MGRN1 suppresses the aggregation and cell death caused by expanded polyglutamine proteins. (A) EGFP-HDQ74 expanded-polyglutamine-expressing cells were co-transfected with MGRN1 and MGRN1-siRNA along with control (pcDNA) plasmid and control siRNA oligonucleotides. After 72 h of transfection, the cells were subjected to quantitative immunofluorescence analysis and immunoblot analysis with MGRN1 and actin antibodies. (B) As described in panel A, the same cells were collected and processed for immunoblotting analysis using anti-GFP, anti-Myc, anti-MGRN1 and anti-actin. (C–D) As described in A and B, EGFP-HDQ74 expanded-polyglutamine-expressing cells were transiently transfected with Myc-MGRN1 (C) plasmid and MGRN1-siRNA (D) oligonucleotides including controls; aggregate formation was counted under a fluorescence microscope at the different times indicated in the figure. The results are the mean ± SD of three independent experiments, each performed in triplicate. *, $p < 0.05$ compared with controls. (E) The toxicity of EGFP-HDQ74 in cells co-expressing Myc-MGRN1 and Hsp70 constructs. Cells were harvested and replated in 96-well tissue-cultured plates. Cell viability was measured by MTT assay. Values are the mean ± SD of two independent experiments, each performed in triplicate. *, $p < 0.05$ compared with control (EGFP-HDQ74 transfected samples). (F) MGRN1 siRNA and control siRNA oligonucleotides were transiently transfected in EGFP-HDQ74 expanded polyglutamine expressing cells. Cell viability was measured by MTT assay. Values are the mean ± SD of two independent experiments, each performed in triplicate. *$p < 0.05$ compared with the control siRNA co-transfected with EGFP-HDQ74 plasmid. (G) Cells were treated with 10 mM BME (β-mercaptoethanol) and exposed to heat stress (HS) 43 °C for 45 min, after treatment cell viability was measured by MTT assay. Values are the mean ± SD of two independent experiments, each performed in triplicate. *, $p < 0.05$ compared with the control (stress-inducing treated) experiment. Cell lysates were also processed for immunoblotting with GFP antibody.

Award (IYBA) scheme (BT/06/IYBA/2012) from the Department of Biotechnology, Government of India. The authors would like to thank Mr. Bharat Pareek and Mr. Sachin Chinchwadkar for their technical assistance and entire lab management during the manuscript preparation. We thank to Dr. Nihar Ranjan Jana (National Brain Research Centre, India) for giving the NeuN antibody. We also thank the following for giving the plasmids: Dr. Teresa M. Gunn (McLaughlin Research Institute Great Falls, Montana, USA) for the MGRN1-GFP and MGRN1 (AVVA)-GFP constructs, Dr. C. Olivares Sánchez and Dr. J.C. García-Borrón (University of Murcia, Campus de Espinardo, Murcia, Spain) for pcDNA3-MGRN1 L (−)-myc plasmid, Dr. Lois Greene (Laboratory of Cell Biology, NHLBI, NIH, Bethesda, MD) for the pEGFP hsp70 construct, Dr. Henry L. Paulson (The University of Michigan Health System, Department of Neurology, Ann Arbor, MI) for pEGFP-C1-Ataxin3Q28 and pEGFP-C1-Ataxin3Q84 constructs, Dr. Douglas T. Golenbock (University of Massachusetts Medical School, Worcester MA) for the pcDNA3-EGFP plasmid, Dr. Wafik S. El-Deiry (Penn State Hershey Cancer Institute, University Drive Hershey, PA) for the pcDNA3-cmyc and Dr. A. Tunnacliffe (Department of Chemical Engineering and Biotechnology, University of Cambridge, Cambridge, UK) for EGFP-HDQ23 and EGFP-HDQ74 constructs.

References

[1] C.A. Ross, M.A. Poirier, Protein aggregation and neurodegenerative disease, Nat. Med. 10 (Suppl.) (2004) S10–S17.
[2] B. Ravikumar, D.C. Rubinsztein, Role of autophagy in the clearance of mutant huntingtin: a step towards therapy? Mol. Aspects Med. 27 (2006) 520–527.
[3] R.R. Kopito, Aggresomes, inclusion bodies and protein aggregation, Trends Cell Biol. 10 (2000) 524–530.
[4] H.Y. Zoghbi, H.T. Orr, Glutamine repeats and neurodegeneration, Annu. Rev. Neurosci. 23 (2000) 217–247.
[5] N.R. Jana, P. Dikshit, A. Goswami, S. Kotliarova, S. Murata, K. Tanaka, N. Nukina, Co-chaperone CHIP associates with expanded polyglutamine protein and promotes their degradation by proteasomes, J. Biol. Chem. 280 (2005) 11635–11640.

[6] R.L. Margolis, C.A. Ross, Expansion explosion: new clues to the pathogenesis of repeat expansion neurodegenerative diseases, Trends Mol. Med. 7 (2001) 479–482.
[7] D. Chhangani, A. Mishra, Protein quality control system in neurodegeneration: a healing company hard to beat but failure is fatal, Mol. Neurobiol. 48 (2013) 141–156.
[8] D. Chhangani, S. Chinchwadkar, A. Mishra, Autophagy coupling interplay: can improve cellular repair and aging? Mol. Neurobiol. (2014), http://dx.doi.org/10.1007/s12035-013-8599-z.
[9] C.J. Cummings, M.A. Mancini, B. Antalffy, D.B. DeFranco, H.T. Orr, H.Y. Zoghbi, Chaperone suppression of aggregation and altered subcellular proteasome localization imply protein misfolding in SCA1, Nat. Genet. 19 (1998) 148–154.
[10] Y. Chai, S.L. Koppenhafer, S.J. Shoesmith, M.K. Perez, H.L. Paulson, Evidence for proteasome involvement in polyglutamine disease: localization to nuclear inclusions in SCA3/MJD and suppression of polyglutamine aggregation in vitro, Hum. Mol. Genet. 8 (1999) 673–682.
[11] B. Ravikumar, R. Duden, D.C. Rubinsztein, Aggregate-prone proteins with polyglutamine and polyalanine expansions are degraded by autophagy, Hum. Mol. Genet. 11 (2002) 1107–1117.
[12] D. Chhangani, N.R. Jana, A. Mishra, Misfolded proteins recognition strategies of E3 ubiquitin ligases and neurodegenerative diseases, Mol. Neurobiol. 47 (2013) 302–312.
[13] D. Chhangani, A.P. Joshi, A. Mishra, E3 ubiquitin ligases in protein quality control mechanism, Mol. Neurobiol. 45 (2012) 571–585.
[14] C.I. Holmberg, K.E. Staniszewski, K.N. Mensah, A. Matouschek, R.I. Morimoto, Inefficient degradation of truncated polyglutamine proteins by the proteasome, EMBO J. 23 (2004) 4307–4318.
[15] D.H. Hyun, M. Lee, B. Halliwell, P. Jenner, Proteasomal inhibition causes the formation of protein aggregates containing a wide range of proteins, including nitrated proteins, J. Neurochem. 86 (2003) 363–373.
[16] S.J. Berke, H.L. Paulson, Protein aggregation and the ubiquitin proteasome pathway: gaining the UPPer hand on neurodegeneration, Curr. Opin. Genet. Dev. 13 (2003) 253–261.
[17] V.I. Korolchuk, F.M. Menzies, D.C. Rubinsztein, Mechanisms of cross-talk between the ubiquitin–proteasome and autophagy–lysosome systems, FEBS Lett. 584 (2010) 1393–1398.
[18] W.X. Ding, H.M. Ni, W. Gao, T. Yoshimori, D.B. Stolz, D. Ron, X.M. Yin, Linking of autophagy to ubiquitin–proteasome system is important for the regulation of endoplasmic reticulum stress and cell viability, Am. J. Pathol. 171 (2007) 513–524.
[19] A. Williams, L. Jahreiss, S. Sarkar, S. Saiki, F.M. Menzies, B. Ravikumar, D.C. Rubinsztein, Aggregate-prone proteins are cleared from the cytosol by autophagy: therapeutic implications, Curr. Top. Dev. Biol. 76 (2006) 89–101.
[20] A.M. Cuervo, Autophagy: in sickness and in health, Trends Cell Biol. 14 (2004) 70–77.
[21] J.L. Webb, B. Ravikumar, J. Atkins, J.N. Skepper, D.C. Rubinsztein, Alpha-synuclein is degraded by both autophagy and the proteasome, J. Biol. Chem. 278 (2003) 25009–25013.
[22] N. Morimoto, M. Nagai, Y. Ohta, K. Miyazaki, T. Kurata, M. Morimoto, T. Murakami, Y. Takehisa, Y. Ikeda, T. Kamiya, K. Abe, Increased autophagy in transgenic mice with a G93A mutant SOD1 gene, Brain Res. 1167 (2007) 112–117.
[23] T. Hara, K. Nakamura, M. Matsui, A. Yamamoto, Y. Nakahara, R. Suzuki-Migishima, M. Yokoyama, K. Mishima, I. Saito, H. Okano, N. Mizushima, Suppression of basal autophagy in neural cells causes neurodegenerative disease in mice, Nature 441 (2006) 885–889.
[24] T. Kabuta, Y. Suzuki, K. Wada, Degradation of amyotrophic lateral sclerosis-linked mutant Cu,Zn-superoxide dismutase proteins by macroautophagy and the proteasome, J. Biol. Chem. 281 (2006) 30524–30533.
[25] O. Chakrabarti, R.S. Hegde, Functional depletion of mahogunin by cytosolically exposed prion protein contributes to neurodegeneration, Cell 137 (2009) 1136–1147.
[26] L. He, X.Y. Lu, A.F. Jolly, A.G. Eldridge, S.J. Watson, P.K. Jackson, G.S. Barsh, T.M. Gunn, Spongiform degeneration in mahoganoid mutant mice, Science 299 (2003) 710–712.
[27] N.R. Jana, E.A. Zemskov, G. Wang, N. Nukina, Altered proteasomal function due to the expression of polyglutamine-expanded truncated N-terminal huntingtin induces apoptosis by caspase activation through mitochondrial cytochrome c release, Hum. Mol. Genet. 10 (2001) 1049–1059.
[28] A. Mishra, S.K. Godavarthi, N.R. Jana, UBE3A/E6-AP regulates cell proliferation by promoting proteasomal degradation of p27, Neurobiol. Dis. 36 (2009) 26–34.
[29] A. Mishra, N.R. Jana, Regulation of turnover of tumor suppressor p53 and cell growth by E6-AP, a ubiquitin protein ligase mutated in Angelman mental retardation syndrome, Cell. Mol. Life Sci. 65 (2008) 656–666.
[30] A. Mishra, M. Maheshwari, D. Chhangani, N. Fujimori-Tonou, F. Endo, A.P. Joshi, N.R. Jana, K. Yamanaka, E6-AP association promotes SOD1 aggresomes degradation and suppresses toxicity, Neurobiol. Aging 34 (2013) (1310 e1311-1323).
[31] A. Mishra, P. Dikshit, S. Purkayastha, J. Sharma, N. Nukina, N.R. Jana, E6-AP promotes misfolded polyglutamine proteins for proteasomal degradation and suppresses polyglutamine protein aggregation and toxicity, J. Biol. Chem. 283 (2008) 7648–7656.
[32] L. Mangiarini, K. Sathasivam, M. Seller, B. Cozens, A. Harper, C. Hetherington, M. Lawton, Y. Trottier, H. Lehrach, S.W. Davies, G.P. Bates, Exon 1 of the HD gene with an expanded CAG repeat is sufficient to cause a progressive neurological phenotype in transgenic mice, Cell 87 (1996) 493–506.
[33] A. Mishra, S.K. Godavarthi, M. Maheshwari, A. Goswami, N.R. Jana, The ubiquitin ligase E6-AP is induced and recruited to aggresomes in response to proteasome inhibition and may be involved in the ubiquitination of Hsp70-bound misfolded proteins, J. Biol. Chem. 284 (2009) 10537–10545.
[34] Y. Chai, J. Shao, V.M. Miller, A. Williams, H.L. Paulson, Live-cell imaging reveals divergent intracellular dynamics of polyglutamine disease proteins and supports a sequestration model of pathogenesis, Proc. Natl. Acad. Sci. U. S. A. 99 (2002) 9310–9315.
[35] S. Chakrabortee, C. Boschetti, L.J. Walton, S. Sarkar, D.C. Rubinsztein, A. Tunnacliffe, Hydrophilic protein associated with desiccation tolerance exhibits broad protein stabilization function, Proc. Natl. Acad. Sci. U. S. A. 104 (2007) 18073–18078.
[36] N.F. Bence, R.M. Sampat, R.R. Kopito, Impairment of the ubiquitin–proteasome system by protein aggregation, Science 292 (2001) 1552–1555.
[37] N. Mizushima, B. Levine, A.M. Cuervo, D.J. Klionsky, Autophagy fights disease through cellular self-digestion, Nature 451 (2008) 1069–1075.
[38] B.Y. Kim, J.A. Olzmann, G.S. Barsh, L.S. Chin, L. Li, Spongiform neurodegeneration-associated E3 ligase Mahogunin ubiquitylates TSG101 and regulates endosomal trafficking, Mol. Biol. Cell 18 (2007) 1129–1142.
[39] P. Chastagner, A. Israel, C. Brou, Itch/AIP4 mediates Deltex degradation through the formation of K29-linked polyubiquitin chains, EMBO Rep. 7 (2006) 1147–1153.
[40] G.K. Tofaris, H.T. Kim, R. Hourez, J.W. Jung, K.P. Kim, A.L. Goldberg, Ubiquitin ligase Nedd4 promotes alpha-synuclein degradation by the endosomal–lysosomal pathway, Proc. Natl. Acad. Sci. U. S. A. 108 (2011) 17004–17009.
[41] D. Chhangani, A. Mishra, Mahogunin ring finger-1 (MGRN1) suppresses chaperone-associated misfolded protein aggregation and toxicity, Sci. Rep. 3 (2013) 1972.
[42] Z. Ying, H. Wang, H. Fan, X. Zhu, J. Zhou, E. Fei, G. Wang, Gp78, an ER associated E3, promotes SOD1 and ataxin-3 degradation, Hum. Mol. Genet. 18 (2009) 4268–4281.
[43] H. Yang, X. Zhong, P. Ballar, S. Luo, Y. Shen, D.C. Rubinsztein, M.J. Monteiro, S. Fang, Ubiquitin ligase Hrd1 enhances the degradation and suppresses the toxicity of polyglutamine-expanded huntingtin, Exp. Cell Res. 313 (2007) 538–550.
[44] Y.C. Tsai, P.S. Fishman, N.V. Thakor, G.A. Oyler, Parkin facilitates the elimination of expanded polyglutamine proteins and leads to preservation of proteasome function, J. Biol. Chem. 278 (2003) 22044–22055.
[45] P. Garyali, P. Siwach, P.K. Singh, R. Puri, S. Mittal, S. Sengupta, R. Parihar, S. Ganesh, The malin–laforin complex suppresses the cellular toxicity of misfolded proteins by promoting their degradation through the ubiquitin–proteasome system, Hum. Mol. Genet. 18 (2009) 688–700.
[46] E.J. Bennett, N.F. Bence, R. Jayakumar, R.R. Kopito, Global impairment of the ubiquitin–proteasome system by nuclear or cytoplasmic protein aggregates precedes inclusion body formation, Mol. Cell 17 (2005) 351–365.
[47] Z. Ortega, M. Diaz-Hernandez, J.J. Lucas, Is the ubiquitin–proteasome system impaired in Huntington's disease? Cell. Mol. Life Sci. 64 (2007) 2245–2257.
[48] Z. Ortega, M. Diaz-Hernandez, C.J. Maynard, F. Hernandez, N.P. Dantuma, J.J. Lucas, Acute polyglutamine expression in inducible mouse model unravels ubiquitin/proteasome system impairment and permanent recovery attributable to aggregate formation, J. Neurosci. 30 (2010) 3675–3688.
[49] J.S. Bett, G.M. Goellner, B. Woodman, G. Pratt, M. Rechsteiner, G.P. Bates, Proteasome impairment does not contribute to pathogenesis in R6/2 Huntington's disease mice: exclusion of proteasome activator REGgamma as a therapeutic target, Hum. Mol. Genet. 15 (2006) 33–44.
[50] C.J. Maynard, C. Bottcher, Z. Ortega, R. Smith, B.I. Florea, M. Diaz-Hernandez, P. Brundin, H.S. Overkleeft, J.Y. Li, J.J. Lucas, N.P. Dantuma, Accumulation of ubiquitin conjugates in a polyglutamine disease model occurs without global ubiquitin/proteasome system impairment, Proc. Natl. Acad. Sci. U. S. A. 106 (2009) 13986–13991.
[51] S. Schipper-Krom, K. Juenemann, E.A. Reits, The ubiquitin–proteasome system in Huntington's disease: are proteasomes impaired, initiators of disease, or coming to the rescue? Biochem. Res. Int. 2012 (2012) 837015.
[52] Q. Ding, J.J. Lewis, K.M. Strum, E. Dimayuga, A.J. Bruce-Keller, J.C. Dunn, J.N. Keller, Polyglutamine expansion, protein aggregation, proteasome activity, and neural survival, J. Biol. Chem. 277 (2002) 13935–13942.
[53] F.M. Menzies, K. Moreau, D.C. Rubinsztein, Protein misfolding disorders and macroautophagy, Curr. Opin. Cell Biol. 23 (2011) 190–197.
[54] M. Kon, A.M. Cuervo, Autophagy: an alternative degradation mechanism for misfolded proteins, Protein Misfolding Diseases: Current and Emerging Principles and Therapies, 2, 2010, p. 113.
[55] F. Levy, K. Muehlethaler, S. Salvi, A.L. Peitrequin, C.K. Lindholm, J.C. Cerottini, D. Rimoldi, Ubiquitylation of a melanosomal protein by HECT-E3 ligases serves as sorting signal for lysosomal degradation, Mol. Biol. Cell 16 (2005) 1777–1787.
[56] D. Silvius, R. Pitstick, M. Ahn, D. Meishery, A. Oehler, G.S. Barsh, S.J. DeArmond, G.A. Carlson, T.M. Gunn, Levels of the Mahogunin Ring Finger 1 E3 ubiquitin ligase do not influence prion disease, PLoS One 8 (2013) e55575.
[57] J. Jiao, K. Sun, W.P. Walker, P. Bagher, C.D. Cota, T.M. Gunn, Abnormal regulation of TSG101 in mice with spongiform neurodegeneration, Biochim. Biophys. Acta 1792 (2009) 1027–1035.
[58] A.W. Dunah, H. Jeong, A. Griffin, Y.M. Kim, D.G. Standaert, S.M. Hersch, M.M. Mouradian, A.B. Young, N. Tanese, D. Krainc, Sp1 and TAFII130 transcriptional activity disrupted in early Huntington's disease, Science 296 (2002) 2238–2243.
[59] A. Goswami, P. Dikshit, A. Mishra, N. Nukina, N.R. Jana, Expression of expanded polyglutamine proteins suppresses the activation of transcription factor NFkappaB, J. Biol. Chem. 281 (2006) 37017–37024.
[60] S.H. Li, A.L. Cheng, H. Zhou, S. Lam, M. Rao, H. Li, X.J. Li, Interaction of Huntington disease protein with transcriptional activator Sp1, Mol. Cell Biol. 22 (2002) 1277–1287.
[61] G. Schaffar, P. Breuer, R. Boteva, C. Behrends, N. Tzvetkov, N. Strippel, H. Sakahira, K. Siegers, M. Hayer-Hartl, F.U. Hartl, Cellular toxicity of polyglutamine expansion proteins: mechanism of transcription factor deactivation, Mol. Cell 15 (2004) 95–105.
[62] T. Shimohata, T. Nakajima, M. Yamada, C. Uchida, O. Onodera, S. Naruse, T. Kimura, R. Koide, K. Nozaki, Y. Sano, H. Ishiguro, K. Sakoe, T. Ooshima, A. Sato, T. Ikeuchi, M. Oyake, T. Sato, Y. Aoyagi, I. Hozumi, T. Nagatsu, Y. Takiyama, M. Nishizawa, J. Goto, I. Kanazawa, I. Davidson, N. Tanese, H. Takahashi, S. Tsuji, Expanded polyglutamine

stretches interact with TAFII130, interfering with CREB-dependent transcription, Nat. Genet. 26 (2000) 29–36.
[63] S.N. Rao, R. Maity, J. Sharma, P. Dey, S.K. Shankar, P. Satishchandra, N.R. Jana, Sequestration of chaperones and proteasome into Lafora bodies and proteasomal dysfunction induced by Lafora disease-associated mutations of malin, Hum. Mol. Genet. 19 (2010) 4726–4734.
[64] B. Ravikumar, C. Vacher, Z. Berger, J.E. Davies, S. Luo, L.G. Oroz, F. Scaravilli, D.F. Easton, R. Duden, C.J. O'Kane, D.C. Rubinsztein, Inhibition of mTOR induces autophagy and reduces toxicity of polyglutamine expansions in fly and mouse models of Huntington disease, Nat. Genet. 36 (2004) 585–595.
[65] P.O. Bauer, A. Goswami, H.K. Wong, M. Okuno, M. Kurosawa, M. Yamada, H. Miyazaki, G. Matsumoto, Y. Kino, Y. Nagai, N. Nukina, Harnessing chaperone-mediated autophagy for the selective degradation of mutant huntingtin protein, Nat. Biotechnol. 28 (2010) 256–263.
[66] S. Sarkar, E.O. Perlstein, S. Imarisio, S. Pineau, A. Cordenier, R.L. Maglathlin, J.A. Webster, T.A. Lewis, C.J. O'Kane, S.L. Schreiber, D.C. Rubinsztein, Small molecules enhance autophagy and reduce toxicity in Huntington's disease models, Nat. Chem. Biol. 3 (2007) 331–338.
[67] M. Jimenez-Sanchez, F. Thomson, E. Zavodszky, D.C. Rubinsztein, Autophagy and polyglutamine diseases, Prog. Neurobiol. 97 (2012) 67–82.

Neurobiology of Disease 86 (2016) 16–28

Contents lists available at ScienceDirect

Neurobiology of Disease

journal homepage: www.elsevier.com/locate/ynbdi

Mahogunin ring finger 1 confers cytoprotection against mutant SOD1 aggresomes and is defective in an ALS mouse model

Deepak Chhangani [a], Fumito Endo [b], Ayeman Amanullah [a], Arun Upadhyay [a], Seiji Watanabe [b], Ribhav Mishra [a], Koji Yamanaka [b,*], Amit Mishra [a,*]

[a] Cellular and Molecular Neurobiology Unit, Indian Institute of Technology Jodhpur, Rajasthan 342011, India
[b] Department of Neuroscience and Pathobiology Research Institute of Environmental Medicine, Nagoya University, Furo-cho, Chikusa-ku, Nagoya 464-8601, Japan

ARTICLE INFO

Article history:
Received 2 June 2015
Revised 21 October 2015
Accepted 18 November 2015
Available online xxxx

Keywords:
Amyotrophic lateral sclerosis
MGRN1
Cytotoxicity
Protein aggregation
SOD1

ABSTRACT

Proteotoxicity of misfolded, disease-causing proteins is deeply implicated in the pathomechanisms for neurodegenerative diseases including copper-zinc superoxide dismutase (SOD1)-linked amyotrophic lateral sclerosis (ALS). However, the precise cellular quality control (QC) mechanisms against aggregation of misfolded mutant SOD1 proteins remain elusive. Here, we found that the Mahogunin ring finger-1 (MGRN1) E3 ubiquitin ligase, which catalyzes mono-ubiquitination to the substrate, was dysregulated in the cellular and mouse models of ALS and that it preferentially interacted with various mutant forms of SOD1. Intriguingly, the motor neurons of presymptomatic ALS mice have diminished MGRN1 cytoplasmic distribution. MGRN1 was partially recruited to mutant SOD1 inclusions where they were positive for p62 and Lamp2. Moreover, overexpression of MGRN1 reduced mutant SOD1 aggregation and alleviated its proteotoxic effects on cells. Taken together, our findings suggest that MGRN1 contributes to the clearance of toxic mutant SOD1 inclusions likely through autophagic pathway, and, most likely, the sequestration of MGRN1 sensitizes motor neurons to degeneration in the ALS mouse model. Furthermore, the present study identifies the MGRN1-mediated protein QC mechanism as a novel therapeutic target in neurodegenerative diseases.

1. Introduction

Amyotrophic lateral sclerosis (ALS) is a fatal adult-onset progressive neurodegenerative disorder that is characterized by the selective death of motor neurons in the spinal cord and cerebral cortex (Bruijn et al., 2004). Dominant mutations in the copper-zinc superoxide dismutase 1(SOD1) gene encoding the SOD1 enzyme are one of the frequent causes of familial ALS (Bruijn et al., 2004; Raoul et al., 2002; Wong et al., 1995). The overexpression of the human *SOD1* gene carrying ALS-linked mutations in mice reproduces the major pathological hallmark of ALS (Gurney et al., 1994). Mutant SOD1 proteins, which are highly ubiquitinated, form insoluble abnormal inclusions with components of the ubiquitin proteasome system (UPS) and autophagy pathway in motor neurons (Banerjee et al., 2010; Cheroni et al., 2009).

The key mechanism of motor neuron death that is linked to mutant SOD1 aggregates remains poorly understood. Recently, it has been shown that supersaturation of the cellular protein is linked to neurodegeneration and aging (Ciryam et al., 2013). Because the UPS facilitates the degradation of mutant SOD1 proteins, the overexpression of mutant SOD1 proteins decreases the elimination capacity of the proteasome system (Allen et al., 2003; Cheroni et al., 2009; Hoffman et al., 1996; Urushitani et al., 2002). Numerous studies have suggested that mutant SOD1 aggregates lead to several critical cellular dysfunctions, such as UPS alterations, endoplasmic reticulum (ER) stress, mitochondrial dysfunction, and oxidative stress (Cheroni et al., 2009; Kikuchi et al., 2006; Lin and Beal, 2006).

Despite knowing that abnormal SOD1 protein aggregation results in a toxic gain of function and contributes to ALS disease progression, it is still not clear how neuronal cells survive under such devastating dysfunctions. One possible cellular response is autophagy. Several lines of evidence have suggested that autophagy activation alleviates mutant SOD1-linked toxic insults (Wong and Cuervo, 2010). SOD1G93A-transgenic mice show numerous microtubule-associated protein 1A/1B-light chain 3 (LC-3)-labeled autophagic vacuoles in the spinal motor neurons (Li et al., 2008). In addition, it has been shown that p62/SQSTM1 recognizes mutant SOD1 proteins through an autophagy-linked lysosomal pathway and promotes their clearance (Gal et al., 2009; Zhang et al., 2007).

Aberrant function of Mahogunin ring finger-1 (MGRN1), a RING domain-containing E3 ubiquitin ligase, causes late-onset spongiform neurodegeneration in mice (He et al., 2003). MGRN1, a unique E3 ligase which catalyzes multi-monoubiquitination to the substrate, and is likely to be involved in the cellular quality control machinery through

* *Corresponding authors.
E-mail addresses: kojiyama@riem.nagoya-u.ac.jp (K. Yamanaka), amit@iitj.ac.in (A. Mishra).
Available online on ScienceDirect (www.sciencedirect.com).

http://dx.doi.org/10.1016/j.nbd.2015.11.017
0969-9961/

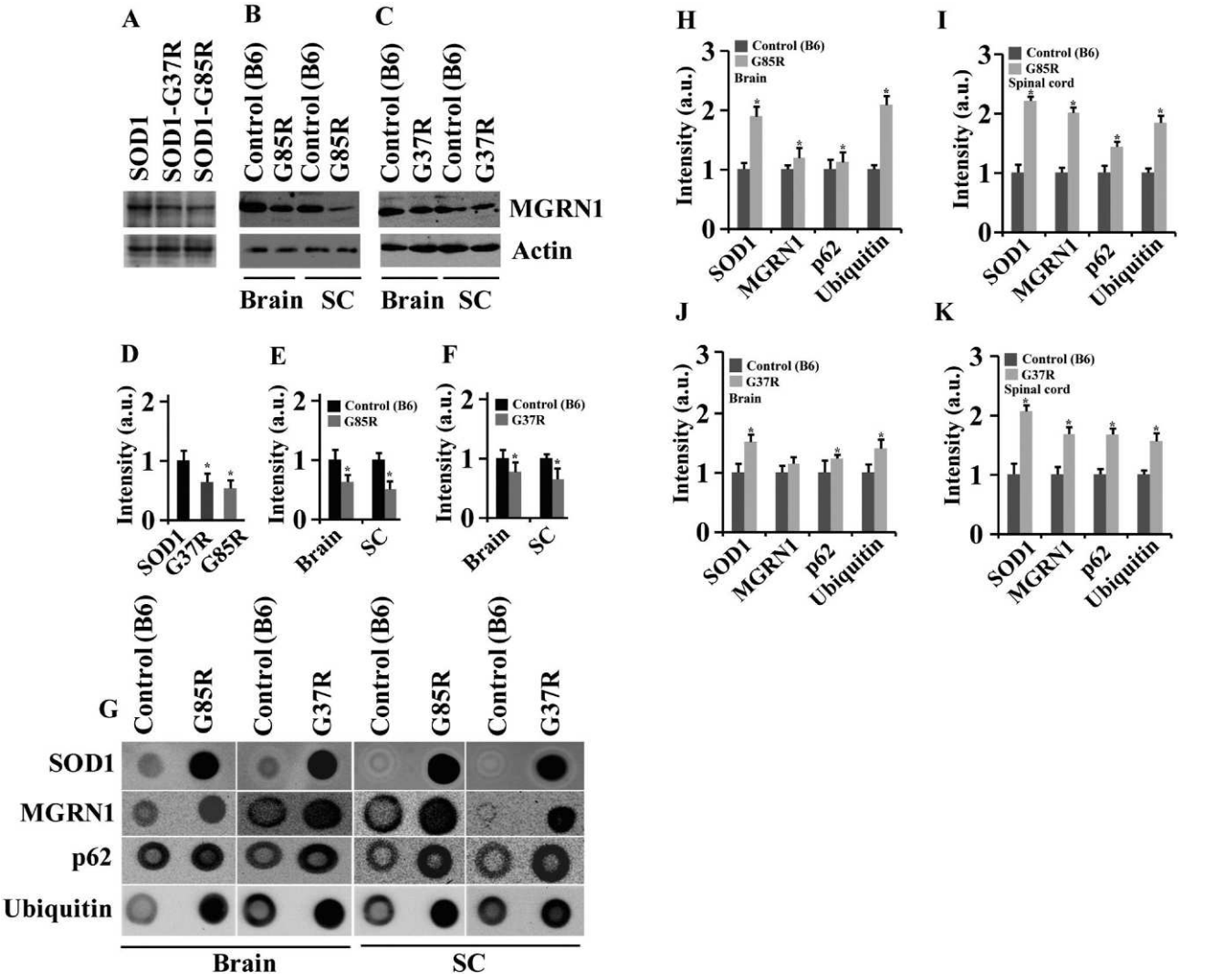

Fig. 1. Mahogunin ring finger-1 (MGRN1) E3 ubiquitin ligase is dysregulated in the cells and mice expressing ALS-linked mutant superoxide dismutase (SOD1) protein. (A) Lysates from COS-7 cells transfected with green fluorescent protein (GFP)-tagged wild-type (WT) and mutant (SOD1G37R and SOD1G85R) SOD1 were analyzed by immunoblotting with anti-MGRN1 and anti-actin antibodies. (B-C) Immunoblotting of MGRN1 in the brain and spinal cord samples of WT (Control: B6) and ALS mice (SOD1G85R and SOD1G37R). (D) As shown in Fig. 1A six well plate cultured cells were used from three independent experiments for quantification. Bar diagram showing the quantification of the band intensities of the wild-type and mutant SOD1-expressing cells and the blots were quantified from three different experiments with NIH Image analysis software. (E–F) Quantification of the band intensities in the immunoblots using brain and spinal cord (SC) lysates of ALS mice (SOD1G85R and SOD1G37R; n = 3 animals) and similar groups (n = 3 animals) of Control (B6) mice. The actin protein levels in each were used for the normalization of each sample. (G) The dot blots that were prepared with the extracts from the brain and SC of WT and early symptomatic ALS mice were detected by immunoassays with anti-SOD1, anti-MGRN1, anti-p62, and anti-ubiquitin antibodies. (H–K) Quantification of the dot-blot results shown in G. The inclusions of various proteins were quantified by a densitometric analysis with NIH image software in WT (control; n = 3 animals) and ALS mice (n = 3 animals) in brain (H, J) and SC (I, K) samples.

proteasome-independent pathway (Chhangani and Mishra, 2013; Chhangani et al., 2014b; Kim et al., 2007). Mice lacking MGRN1 function exhibit dysregulation of the mitochondrial pathway and neurodegeneration (Sun et al., 2007). Downregulation of MGRN1 disturbs endo-lysosome molecular trafficking of epidermal growth factor and null mice of MGRN1 indicate that MGRN1-deficient neurons are more prone for high vulnerable risk in comparison of other cells due to abnormal endosomal trafficking (Kim et al., 2007). Recently it has also been demonstrated that MGRN1 interacts with transmembrane (^{Ctm}PrP) and toxic (cyPrP) prion disease proteins; depletion of MGRN1 affects lysosomal morphology and leads to neurodegeneration likely due to such improper sequestration (Chakrabarti and Hegde, 2009). MGRN1 interacts with several proteins such as expanded polyglutamine proteins (Chhangani et al., 2014b), molecular chaperone (Chhangani and Mishra, 2013), α-tubulin (Srivastava and Chakrabarti, 2014), MC1R/MC2R (Cooray et al., 2011; Perez-Oliva et al., 2009), cyPrP/^{Ctm}PrP (Chakrabarti and Hegde, 2009), TSG 101 (Kim et al., 2007), and NEDD4 (Gunn et al., 2013). Under such crucial biological interactions it is plausible that a loss of function or depletion of MGRN1 can cause multifactorial defects in cells and generate various pathological states in important physiological events. As recently we reviewed (Upadhyay et al., 2015) and previous studies also indicated strong implications of MGRN1 in neuropathobiological mechanisms. How misfolded or aggregated proteins affect physiological function of MGRN1 and disturb normal localization at the site of proper recruitment is a crucial question. However, the role of MGRN1 in neurodegenerative diseases has not been clarified. Although abnormal protein accumulation is a prominent feature of neurodegenerative diseases, how the sequestration or loss of function of MGRN1 contributes to neurodegeneration is not known.

In our present study, we found MGRN1 dysregulation in cellular and mouse models of ALS. MGRN1 interacts with normal and mutant SOD1 proteins in cells. The motor neurons showed diminished MGRN1 cytoplasmic labeling in presymptomatic mutant SOD1 mice. MGRN1 was partially recruited to mutant SOD1 inclusions,

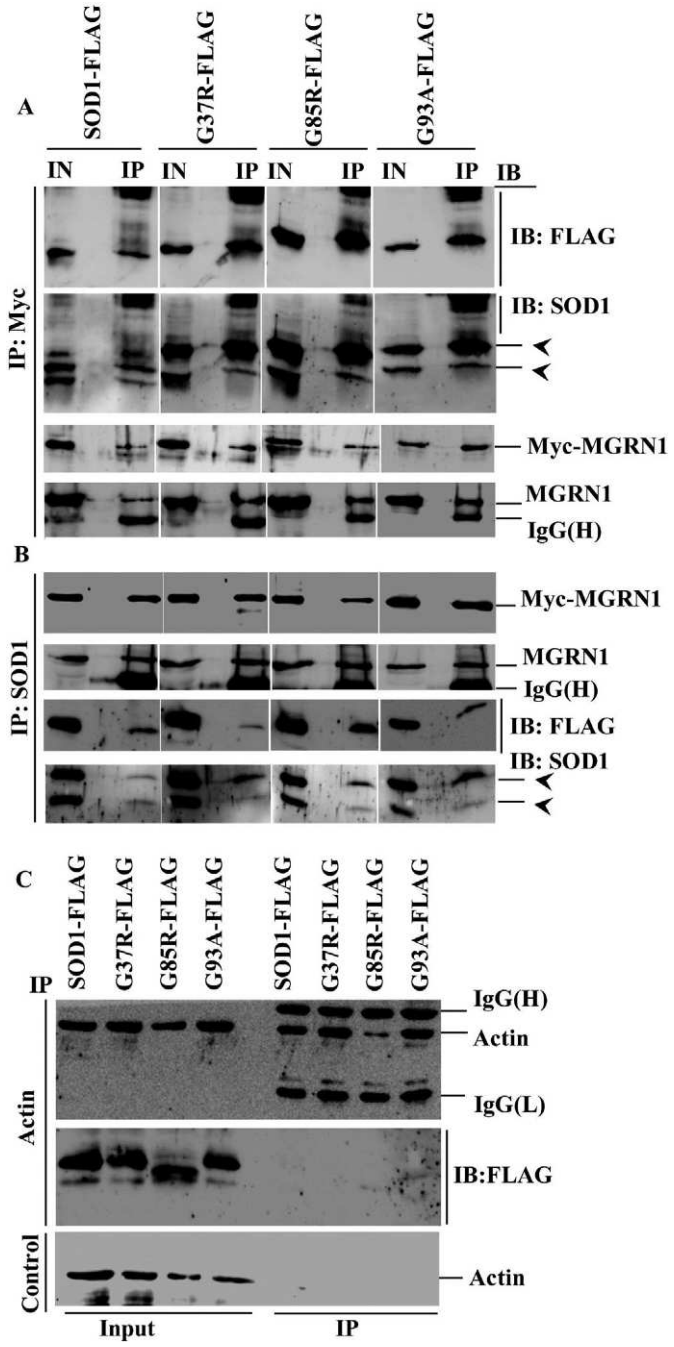

Fig. 2. MGRN1 interacts with wild-type and mutant SOD1 proteins. (A) MGRN1 and SOD1 co-immunoprecipitation (CO-IP). Lysates were prepared from COS-7 cells transfected with Myc-MGRN1 and FLAG-tagged wild-type (SOD1) and mutant (SOD1G37R, SOD1G85R, and SOD1G93A) SOD1 plasmids. Transfected cells were processed for CO-IP with an anti-Myc antibody. After the CO-IP, the blots were probed with anti-FLAG, anti-SOD1, anti-Myc, or anti-MGRN1 antibodies. (B) As described above, the same cell lysates were used for CO-IP with an SOD1 antibody, and immunoblotting was performed with anti-Myc, anti-MGRN1, anti-FLAG, or anti-SOD1 antibodies. The arrowheads represent exogenous (upper) and endogenous (lower) SOD1. (C) As an immunoprecipitation control, COS-7 cells were expressed with the above-described constructs, and, after 48 h, the cell lysates were prepared and immunoprecipitated with an anti-actin antibody or Protein G agarose (control). The pulled-down products and cell lysates were used for immunoblotting and sequentially probed with anti-actin and anti-FLAG antibodies.

which were positive for p62 and Lamp2 in the spinal motor neurons of ALS mice. Finally, MGRN1 alleviates the cytotoxicity mediated by abnormal inclusions of mutant SOD1 and thus, exerts a cytoprotective effect. Overall, these findings suggest that an MGRN1-mediated protein quality control mechanism alleviates the mutant SOD1-linked proteotoxicity likely through autophagic pathway.

2. Materials and methods

2.1. Materials

3-(4,5-Dimethylthiazol-2-yl)-2,5-diphenyltetrazolium bromide (MTT), Bafilomycin A1 (Baf), chloroquine, cycloheximide, MGRN1-specific siRNA oligonucleotides, and all cell culture reagents were obtained from Sigma-Aldrich Co. LLC (St. Louis, MO, USA). The protein G-agarose beads were obtained from Roche Applied Science (Indianapolis, IN, USA). The TRIzol reagent, Lipofectamine®2000, OptiMEM, and reverse transcription-polymerase chain reaction (RT-PCR) kits were purchased from Life Technologies Corporation (Grand Island, NY, USA). The pcDNA™ 3.1 plasmid was purchased from Life Technologies Corporation. The pEGFP-Hsp70 (Addgene 15215), pcDNA3-EGFP (Addgene 13031), pcDNA3-cmyc (Addgene 16011), pF148 pSOD1G37RAcGFP1 (Addgene 26409), and pF150 pSOD1G93AAcGFP1 (Addgene 26411) plasmids were purchased from Addgene (Cambridge, MA, USA). The wild-type and mutant SOD1 plasmids have been described elsewhere (Mishra et al., 2013).

2.2. Primary and secondary antibodies

The monoclonal green fluorescent protein (GFP-11814460001) antibody was purchased from *Roche Applied Science*. The monoclonal anti-Hsp70 (sc-32239), polyclonal anti-SOD1 (sc-11407), polyclonal anti-GFP (sc-8334), polyclonal anti-MGRN1 (sc-160518), monoclonal anti-ubiquitin (sc-58448), and siRNA-MGRN1 oligonucleotides were purchased from *Santa Cruz Biotechnology*, *Inc.* (*Santa Cruz*, *CA*, *USA*). Anti-FLAG (F7425), polyclonal anti-MGRN1 (HPA007653), monoclonal anti-p62/SQSTM1 (WH0008878M1), anti-c-Myc (M4439), anti-actin (A2066), and anti-Lamp2 (SAB1402250) were obtained from *Sigma-Aldrich Co. LLC*. Polyclonal anti-ubiquitin (Z0458) was purchased from *Dako* (*Glostrup*, *Denmark*). Multi ubiquitin antibody was purchased from *MEDICAL & BIOLOGICAL LABORATORIES* (*MBL*: *Nagoya*, *Japan*). The anti-human SOD1 antibody (M062-3) was obtained from *MBL International* (*Woburn*, *MA*, *USA*). Monoclonal misfold SOD1-specific antibody (clone C4F6) was obtained from *MediMabs* (*Montreal*, *Canada*). Anti-mouse IgG-fluorescein isothiocyanate (FI-2000) (IgG-FITC) and IgG-rhodamine (TI-2000), anti-rabbit IgG-FITC (FI-1000) and IgG-rhodamine (TI-1000), and the horseradish peroxidase-conjugated anti-mouse (PI-2000), anti-rabbit-(PI-1000), and anti-goat IgGs (PI-9500) were purchased from *Vector Laboratories*, *Inc.* (*Burlingame*, *CA*, *USA*). The Zenon® Secondary Detection-Based Zenon® Alexa Fluor® 350 Mouse IgG_1 Labeling Kit (Z-25,000); was obtained from *Life Technologies Corporation*.

2.3. Cell culture, transfection, and cell viability assay

COS-7 cells and 293T cells were maintained at 37 °C and 5% CO_2 in Dulbecco's modified Eagle's medium (Sigma-Aldrich Co. LLC) with 100 U/mL penicillin and 100 μg/mL streptomycin and 10% heat-

Fig. 3. Colocalization of MGRN1 and SOD1 aggregates in motor neurons in the spinal cord of ALS-transgenic (SOD1G85R) mice. (A–D) Anterior horn spinal cord slices of presymptomatic SOD1G85R-transgenic mice (8 months old; n = 3 animals) were processed for double-immunofluorescence staining with 8-month-old non-transgenic mice (control B6; n = 3 animals). The superimposed images demonstrate the colocalization of MGRN1 with SOD1- (A), Lamp2- (B), Ubiquitin- (C), and p62- (D) positive aggregates. A rhodamine-conjugated secondary antibody was used to label MGRN1, and a FITC-conjugated secondary antibody was used to label SOD1, Lamp2, ubiquitin, and p62. The arrowheads indicate colocalization. Scale bar, 20 μm.

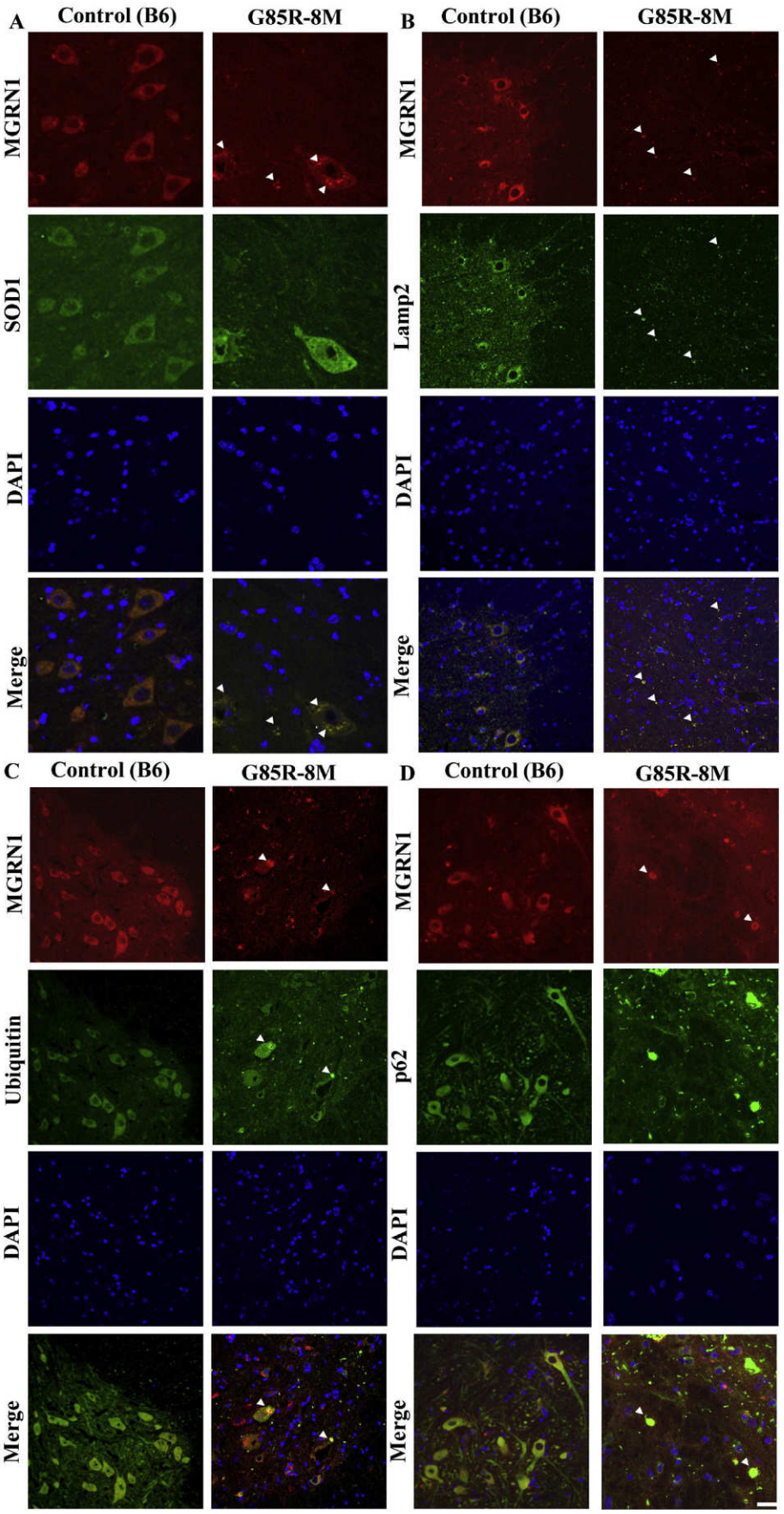
A
Control (B6)
G85R-8M
MGRN1
SOD1
DAPI
Merge
B
Control (B6)
G85R-8M
MGRN1
Lamp2
DAPI
Merge
C
Control (B6)
G85R-8M
MGRN1
Ubiquitin
DAPI
Merge
D
Control (B6)
G85R-8M
MGRN1
p62
DAPI
Merge

inactivated fetal bovine serum. Cells were transiently transfected with various constructs as described in the figures, and the Lipofectamine®2000 transfection reagent was used according to the manufacturer's protocol for transfections. The cells were treated with reagents at 37 °C, at a subconfluent density; the reagents were added drop-wise into the 6-well tissue culture plates. The cells were processed for different immunofluorescence stainings and immunoblotting experiments after 48 h when the transfection efficiency was about 70%. Cell viability was assessed with MTT, as described previously (Mishra et al., 2013; Mulherkar et al., 2009).

2.4. Immunocytochemistry technique, counting of aggregates, and statistical analysis

COS-7 cells were plated into 2-well chamber slides and transiently transfected as described above. Transfected cells were processed for double immunolabeling as follows. Cells were rinsed 4 times with phosphate-buffered saline (PBS), fixed with 4% paraformaldehyde, permeabilized with 0.3% Triton X-100, and blocked with 2% goat serum for 1 h. The cells were then incubated with primary antibodies (1:500) overnight at 4 °C. The next day, the cells were washed three times with Tris-buffered saline with Tween (TBST), and a fluorochrome-conjugated secondary antibody was used for 2 h. The cells were then washed 4 times with PBS, which was followed by 4′, 6-diamidino-2-phenylindole (DAPI) staining. After mounting with Vectashield mount medium (Vector Laboratories, Burlingame, CA), these cells were visualized with a fluorescence microscope (Leica DM 6000B, Leica Microsystems GmbH, Wetzlar, Germany). For counting aggregates, about 500 cells were observed, and aggregate formation was counted manually under a fluorescence microscope. Cells retaining more than one aggregate were counted as having a single inclusion or aggregate. The statistical significance for comparisons of the means of more than two groups, one-way ANOVA was used. In some experiments the statistical analyses between the groups and intergroup comparisons were determined with Student's *t*-tests and Microsoft Excel software..

2.5. Coimmunoprecipitation and immunoblotting experiment

COS-7 cells were transiently transfected with different constructs. After 48 h of transfection, the cells were rinsed with PBS, and placed used on ice for 45 min with Nonidet P-40 lysis buffer (50 mM Tris, pH 7.4, 150 mM NaCl, 1% Nonidet P-40, and complete protease inhibitor mixture), to prepare the lysate. Cell lysates were briefly sonicated twice and centrifuged for 10 min at 10,000 ×*g* at 4 °C, and the supernatants (total protein lysates) were used for immunoprecipitation, as described previously (Mishra et al., 2009). In each immunoprecipitation experiment, 200 μg of protein in 0.2 mL of Nonidet P-40 lysis buffer was used for a pull-down experiment and incubated for 4 h with the desired antibody. After the coimmunoprecipitation experiment, the samples were separated with sodium dodecyl sulfate-polyacrylamide gel electrophoresis (SDS-PAGE). The gels were transferred onto nitrocellulose membranes and incubated under blocking buffer [5% skim milk in TBST (50 mM Tris, pH 7.5, 0.15 M NaCl, 0.05% Tween)] for 1 h. Homogenate extracts from the brain and spinal cord of wild-type and ALS mice were used for a dot-blot analysis on membrane-filter assays, as previously described (Wanker et al., 1999). After blocking, the membranes were incubated with different primary antibodies in TBST and then processed for secondary antibody incubation. All of the blots were developed with ECL substrate. All primary antibodies were used for immunoblotting at a 1:500 dilution.

2.6. Degradation assay, RT-PCR analysis, and RNA interference experiments

COS-7 cells were plated in 6-well plates and transiently cotransfected with wild-type and mutant SOD1 constructs along with MGRN1 plasmids. Forty-eight h after transfection, the cells were incubated for 4 h with a cycloheximide solution (15 μg/mL). The proteins in the cell lysate were separated by SDS-PAGE and processed for the immunoblot analysis. The blots were incubated with the appropriate primary antibodies. Quantification of the band intensities of the immunoblots was performed with NIH Image analysis software. Actin was used to normalize the data. For the RT-PCR analysis, total RNA was isolated from the transiently transfected cells using TRIzol reagent, and, then, semi-quantitative RT-PCR was performed with MGRN1-specific and β-actin-specific primers. The details of the RT-PCR conditions were previously described (Chhangani and Mishra, 2013). To deplete the endogenous MGRN1 from the cells, the cells were plated in 6-well tissue culture plates. RNA interference experiments were conducted with transiently transfected MGRN1-siRNA or Control-siRNA oligonucleotides. Transfected cells were collected for RNA isolation, and a RT-PCR analysis was performed, as explained above. Some cells were collected, and the lysate was processed for the immunoblot analysis with a MGRN1 antibody.

2.7. Transgenic mice and fluorescent immunohistochemical staining of spinal cord sections

SOD1-transgenic mice [LoxSOD1G37R (Boillee et al., 2006), SOD1G85R (Bruijn et al., 1997), and SOD1G93A (Gurney et al., 1994)] have been described previously. All animal experiments were conducted with the approval of the Animal Care Committee of Nagoya University and were in accordance with their requirements. Presymptomatic and symptomatic ALS-transgenic mice (n = 3) and similar groups (n = 3) of Control (B6) mice were perfused with sterile PBS, which was followed by 4% paraformaldehyde in PBS. For the double-immunofluorescence labeling, lumbar spinal cords were dissected and fixed with 4% paraformaldehyde in phosphate buffer, treated (for cryoprotection) with 30% sucrose for at least 18 h at 4 °C, and frozen in mounting medium (Yamanaka et al., 2008). Cryosections (20 μm) were directly mounted on the slides, probed with primary antibodies, and later incubated with a fluorescent-conjugated secondary antibodies. Lumbar spinal motor sections were mounted with Prolong antifade reagent and observed on a confocal microscope (LSM700 exciter, Carl Zeiss AG, Oberkochen, Germany), and nuclear staining was detected by DAPI. For quantification of MGRN1-immunoreactivity in the lumbar ventral large neurons, mean fluorescence intensities (MFI) within cell bodies of large neurons (major axis > 20 μm) in the anterior horn area were measured using ZEN software (Carl Zeiss, Germany). The neuronal MFI was normalized to that of the ipsilateral posterior horn area in the same section.

3. Results

3.1. Dysregulation of MGRN1 in ALS-linked transgenic mice prior to neurodegeneration

To test whether the endogenous MGRN1 E3 ubiquitin ligase was dysregulated by mutant SOD1 proteins, we first examined the expression levels of MGRN1 in cultured cells expressing mutant forms of SOD1 proteins. We observed that the endogenous levels of MGRN1 were depleted in the cells expressing mutant SOD1G37R and SOD1G85R proteins and not in the cells expressing wild-type SOD1

Fig. 4. Immunoreactivity of MGRN1 and its recruitment to SOD1 inclusions in motor neurons of ALS-transgenic (SOD1G93A) mice. (A–D) Spinal cord anterior horn sections of 5-month-old symptomatic ALS-transgenic (SOD1G93A) mice (n = 3 animals) and non-transgenic age-matched controls (n = 3 animals) were processed for double-immunolabeling with MGRN1 and SOD1- (A), Lamp2- (B), Ubiquitin- (C), or p62- (D) positive inclusions. MGRN1 was detected with a rhodamine-conjugated secondary antibody, and the other proteins (SOD1, Lamp2, ubiquitin, and p62) were observed with a FITC-conjugated secondary antibody. The arrowheads indicate the overlay (yellow) of dual-positive inclusions. Scale bar, 20 μm.

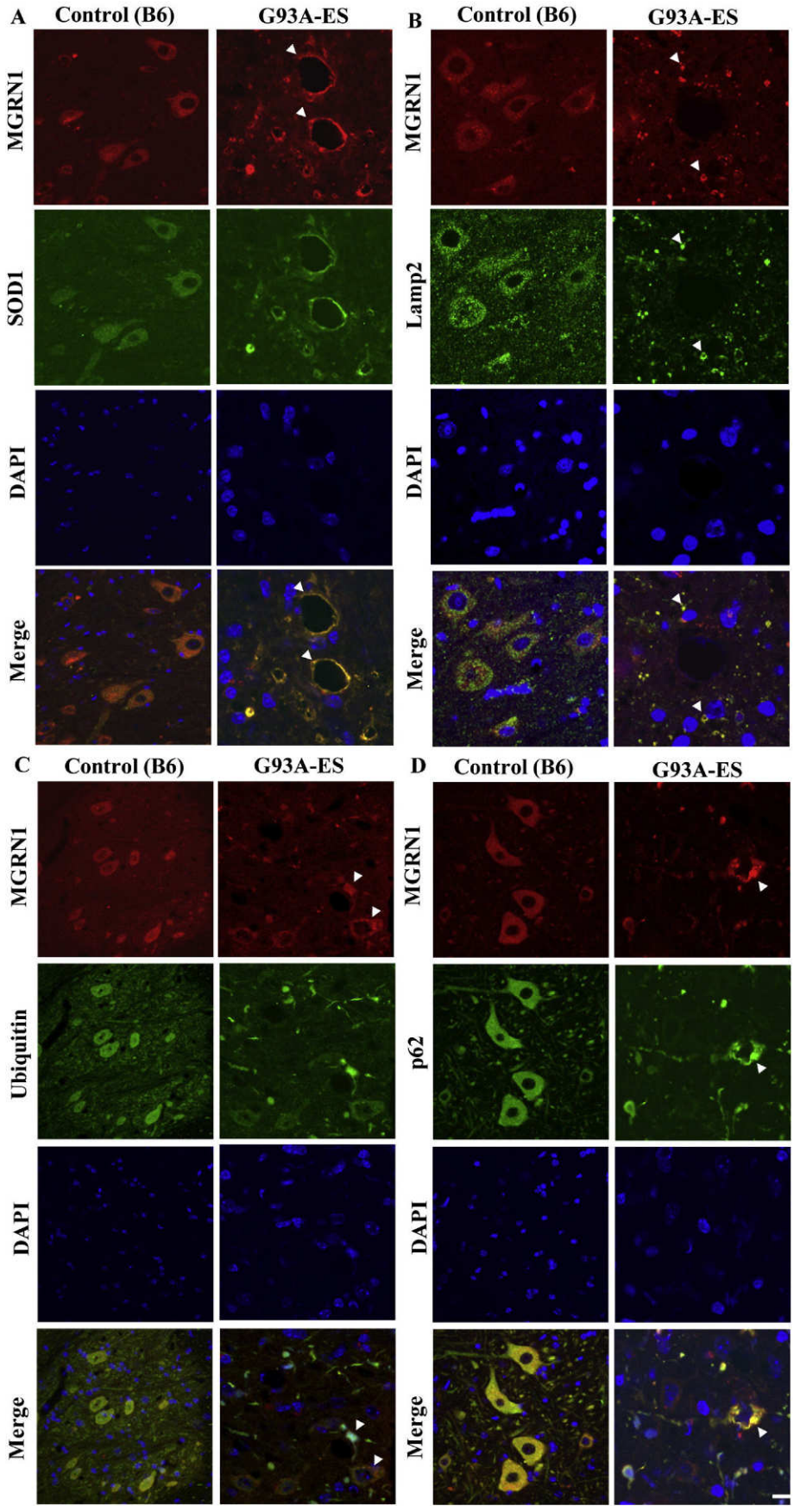
A
Control (B6)
G93A-ES
MGRN1
SOD1
DAPI
Merge
B
Control (B6)
G93A-ES
MGRN1
Lamp2
DAPI
Merge
C
Control (B6)
G93A-ES
MGRN1
Ubiquitin
DAPI
Merge
D
Control (B6)
G93A-ES
MGRN1
p62
DAPI
Merge

protein (Fig. 1A). Mutant SOD1-overexpressing cells showed about a 0.4-fold decrease in the endogenous levels of MGRN1 (Fig. 1D). To further examine alteration of MGRN1 levels in vivo, we investigated the endogenous levels of MGRN1 in ALS-linked SOD1G37R (12 month old)- and SOD1G85R (10 month old)-transgenic mice. We observed that the protein levels of MGRN1 were reduced by about half in both the spinal cord and brain samples of SOD1G37R- and SOD1G85R-transgenic mice in comparison to wild-type control mice of the same age (Fig. 1B, C, E and F). Previous work showed that ubiquitin, proteasomes, and Hsc-70 are positively stained with the neuronal SOD1 inclusions of three different ALS mouse models (G37R, G85R, and G93A SOD1) (Watanabe et al., 2001). Therefore, we hypothesized that the aggregation of misfolded SOD1-aggregated species in ALS-transgenic mice might sequester and coaggregate MGRN1 and deplete its endogenous levels compared to normal mice. To address this question, we performed a dot-blot analysis with homogenate extracts from the brain and spinal cord of wild-type (control) and ALS mice. MGRN1 and other proteins such as SOD1, ubiquitin, and p62 were found to form aggregates in the brains and spinal cords of ALS-transgenic mice (Fig. 1G). Quantification of these dot-blot analyses suggested that MGRN1 strongly aggregated with ubiquitin, p62, and mutant SOD1 proteins in the brains and spinal cords of ALS-transgenic mice (Fig. 1H–K).

3.2. MGRN1 interacts with wild-type and mutant SOD1 proteins

Our initial in vitro and in vivo observations suggested that MGRN1 was sequestered with mutant SOD1 inclusions presumably through their mutual interactions. To determine if MGRN1 interacted with normal and mutated SOD1 proteins, we first conducted a detailed co-immunoprecipitation experiment. FLAG-tagged SOD1, SOD1G37R, SOD1G85R, or SOD1G93A, and Myc-tagged MGRN1 constructs were separately co-transfected into COS-7 cells, and immunoprecipitation was then performed with an anti-Myc antibody. Immunoblots were obtained from the co-immunoprecipitated species and probed with anti-FLAG, anti-SOD1, anti-Myc, and anti-MGRN1 antibodies. As shown in Fig. 2A, MGRN1 preferentially interacted with exogenous mutant SOD1 proteins compared to wild-type endogenous SOD1. To further confirm this interaction, we performed a reverse co-immunoprecipitation analysis. The same cell lysates were used to pull down SOD1 with an anti-SOD1 antibody. Detection of proteins in the precipitates was then performed sequentially with anti-Myc, anti-MGRN1, anti-FLAG, and anti-SOD1 antibodies. Both the wild-type and mutant forms of SOD1 proteins interacted with endogenous as well as exogenous MGRN1 (Fig. 2B). Lastly, we performed various control immunoprecipitation experiments; the cell lysates that were used earlier were separately pulled down by anti-actin or protein G agarose only, and the blots were developed with anti-actin and anti-FLAG antibodies (Fig. 2C). These observations suggested the possible molecular pathophysiological relevance and interaction of MGRN1 with wild-type and mutant SOD1 proteins, and they supported our initial observation of MGRN1 dysregulation in the ALS-transgenic mouse model.

3.3. MGRN1 is sequestered in the spinal motor neurons of presymptomatic and symptomatic mutant SOD1 transgenic mice ALS SOD1G85R- and onset ALS SOD1G93A-transgenic mice

Abnormal SOD1 accumulation and dysregulation of oxidative phosphorylation have been observed in the mitochondria of symptomatic ALS mice (Liu et al., 2004; Mattiazzi et al., 2002; Vijayvergiya et al., 2005). On the other hand, the loss of MGRN1 function has been shown to result in mitochondrial dysfunction and neurodegeneration in MGRN1 null-mutant mice (Sun et al., 2007). The findings of these studies and our current observations of dysregulated endogenous levels of MGRN1 in mutant SOD1-expressing cells and mice may represent a triggering factor in the onset of the disease. This prompted us to further investigate whether the sequestration of MGRN1 was observed in the spinal motor neurons of presymptomatic ALS-transgenic mice. In order to determine the localization of MGRN1, we performed a detailed immunohistochemical profile of MGRN1, and other critical proteins, such as SOD1, Lamp2, ubiquitin, and p62, in the lumbar spinal cord of both wild-type and presymptomatic ALS-transgenic mice. MGRN1 immunoreactivities were predominantly observed in the cytoplasm of motor neurons in the spinal cord of the control (non-transgenic) mice. The spinal cord sections of ALS SOD1G85R (Fig. 3) and SOD1G93A-transgenic (Fig. 4) mice demonstrated cytoplasmic inclusions with MGRN1 immunostaining, which was greatly diminished and colocalized with mutant SOD1 (Fig. 3A & Fig. 4A). As shown in Figs. 3 and 4, mutant SOD1 aggregates showed positive double immunofluorescence staining for MGRN1 and various critical components of proteolytic pathways, such as ubiquitin, Lamp2, and p62 inclusion bodies, in the same set of spinal cord samples. To further examine whether misfolded SOD1 species are involved in dysregulated MGRN1 expression in spinal motor neurons, we performed immunostaining using misfolded SOD1-specific antibody, C4F6. MGRN1 was partially co-localized with misfolded SOD1G93A proteins at onset of disease (Fig. 5A). Abnormal accumulation of MGRN1 was observed both in axons and somata of the neurons. Despite of MGRN1 aggregation occasionally observed, the overall signal intensities of MGRN1 in the somata of anterior horn neurons were significantly diminished before the onset of the disease in SOD1G85R mice (Fig. 5B, C), suggesting that depletion of functional MGRN1 in the neurons of mutant SOD1 mice. Altogether, these immunohistochemical observations suggested that MGRN1 levels were lower in presymptomatic and onset ALS-transgenic mice and that it was partially mislocalized with aberrant SOD1 macromolecular aggregates.

3.4. MGRN1 overexpression reduces the steady-state levels of mutant SOD1 proteins and mitigates their aggregation in cells

In cells, most abnormal proteins are selectively targeted by both proteasome and autophagy pathways (Chhangani et al., 2014a). Moreover, these aberrant proteins are ubiquitinated and positive for various components of the cellular quality control pathway (Chhangani et al., 2013). In our current study, we demonstrated the partial recruitment of MGRN1 with mutant SOD1 proteins in presymptomatic and symptomatic ALS-transgenic mice. Therefore, we speculated that such an association could promote the degradation of mutant SOD1 proteins in cells. Because MGRN1 targets TSG101 for multiple mono-ubiquitination through a proteasomal-independent pathway (Kim et al., 2007), we next performed an immunocytochemical analysis of the cells and observed that chloroquine-mediated autophagy inhibition induced the colocalization of endogenous MGRN1 with inclusions of SOD1G37R-YFP and SOD1G85R-YFP abnormal proteins (Fig. 6A—D). In order to determine whether MGRN1 influences mutant SOD1 protein levels in mammalian cells, we transiently cotransfected cells with control and MGRN1 plasmids along with wild-type and mutant SOD1G93A constructs and treated them with cycloheximide to inhibit protein synthesis, and the levels of wild-type and mutant SOD1 protein over time were analyzed with an immunoblot analysis. The overexpression of MGRN1 reduced the steady-state levels of mutant SOD1G93A protein compared to wild-type SOD1 protein in cells, and, moreover, degradation of SOD1 proteins was retarded in the presence of Bafilomycin, an inhibitor for autophagy (Fig. 6E—H).

To examine whether MGRN1 preferentially targets mutant SOD1 protein in MGRN1 activity dependent manner, we coexpressed wild-type SOD1 and SOD1G93A mutant constructs along with MGRN1 or the catalytically inactive form MGRN1^{AVVA} plasmids in the cells; some cells were treated with 50 nM Baf (Fig. 7A, B). We found that the overexpression of MGRN1 significantly reduced the levels of mutant SOD1G93A protein compared to wild-type SOD1 (Fig. 7A, B). In contrast, no significant decrease in the mutant SOD1G93A contents was detected in the catalytically inactive form of the MGRN1-transfected cells.

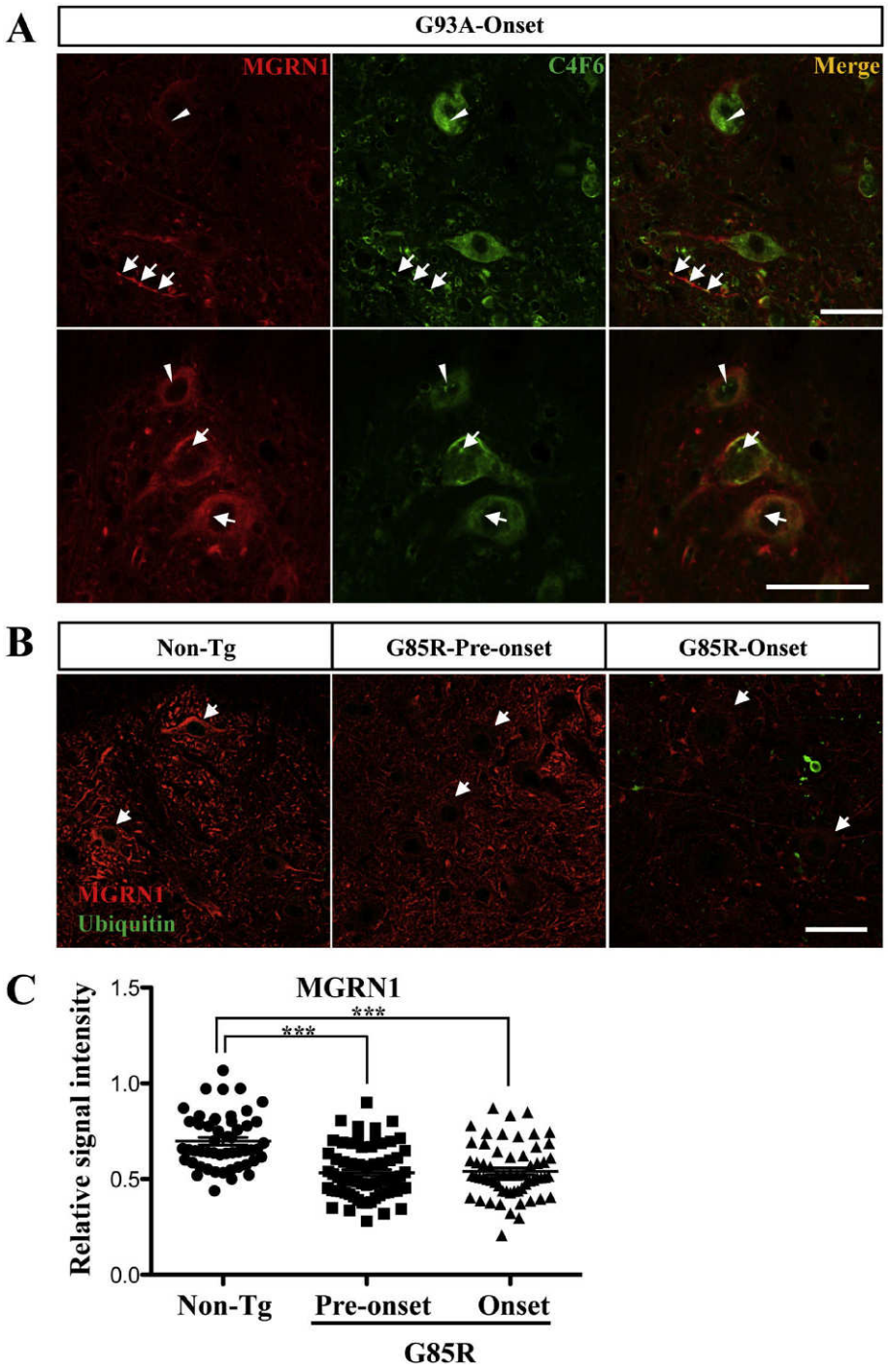

Fig. 5. MGRN1 partially colocalizes with misfolded mutant SOD1 inclusions and decreases in the motor neurons of mutant SOD1 mice. (A) Representative images show the lumbar ventral horn sections of onset (3.5-month-old) $SOD1^{G93A}$ mice stained for MGRN1 (red), C4F6 (green), and the merged image. C4F6-positive inclusions positive (arrows) or negative (arrowheads) for MGRN1 are indicated. Scale bars; 50 μm. (B) Representative images show the lumbar ventral horn sections of non-transgenic, pre-onset (3-month-old), and onset (10-month-old) $SOD1^{G85R}$ mice stained for MGRN1 (red) and multi-ubiquitin (green). Arrows indicate the large neurons in the ventral horns. Scale bars; 50 μm. (C) Relative signal intensities of MGRN1 in the somata of the lumbar ventral large neurons of non-transgenic (n = 2, 51 neurons), pre-onset (3-month-old, n = 2, 67 neurons), and onset (10- or 11-month-old, n = 2, 61 neurons) $SOD1^{G85R}$ mice are shown. Mean signal intensities of the somata of ventral large neurons relative to that of the posterior column are plotted. Error bars denote SEM. $^{***}p < 0.001$.

Treatment with Baf further stabilized the degradation of abnormal SOD1G93A protein, suggesting that MGRN1 facilitated SOD1G93A clearance through the autophagy pathway. The current observations suggested that there were multiple routes of mutant SOD1 protein degradation specifically when the accumulation of abnormal SOD1 proteins impaired the proteasomal functions of cells. To confirm the degradation of other mutant SOD1 species by MGRN1, COS-7 cells were transiently transfected with SOD1G37R and MGRN1-GFP or $MGRN1^{AVVA}$-GFP and processed for immunofluorescence. Compared to $MGRN1^{AVVA}$-GFP-inactive mutants, MGRN1-GFP-positive cells retained very few diffuse inclusions (Fig. 7C—F). Next, we tested the effects of the overexpression (Fig. 7G) and knockdown (Fig. 7H) of MGRN1 on SOD1 aggregate formation. In the cells expressing SOD1G37R-YFP, the overexpression of MGRN1 decreased the number of aggregates, whereas the knockdown of MGRN1 increased aggregate formation in the cells. Taken together, these findings indicate that

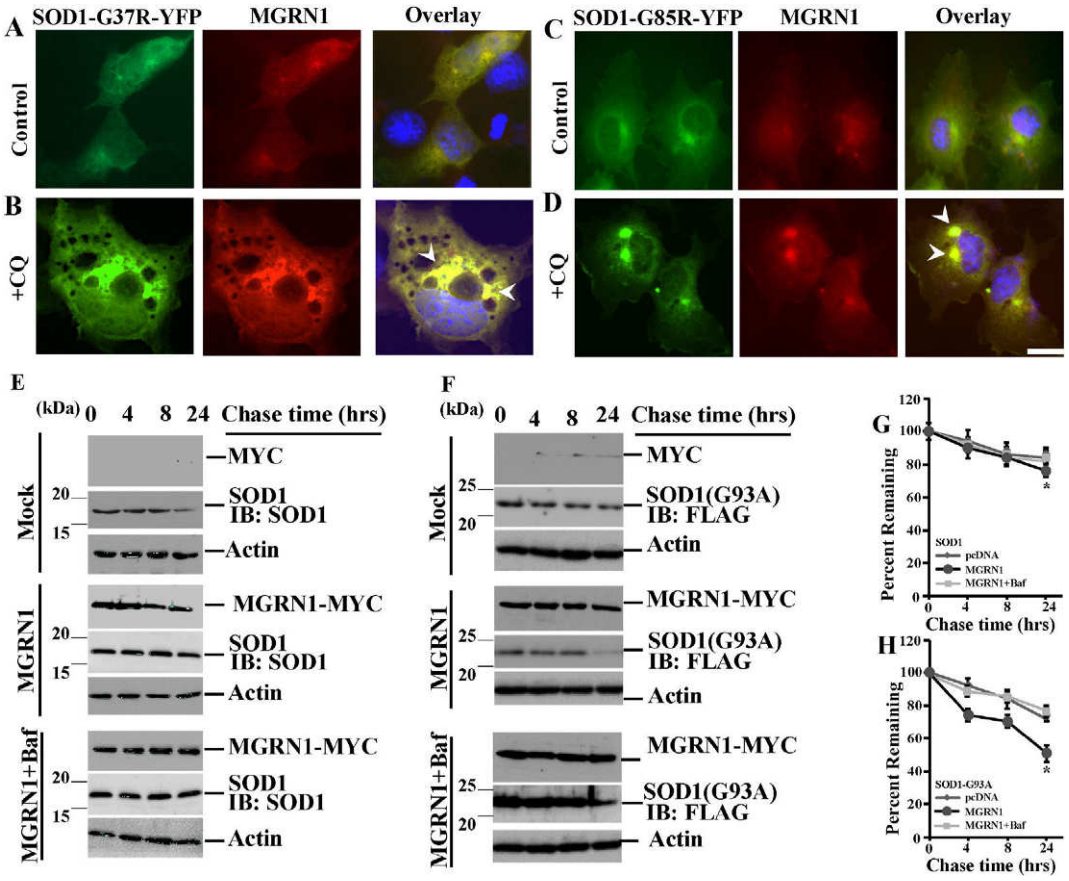

Fig. 6. MGRN1 is associated with mutant SOD1 aggregates and reduces the steady-state levels of mutant SOD1 protein. (A-D) COS-7 cells were transfected with mutant SOD1G37R-YFP (A and B) and SOD1G85R-YFP (C and D) plasmids, and some transfected cells were treated with 30 μM of chloroquine (CQ) (B, D). A rhodamine-conjugated secondary antibody was used to detect endogenous MGRN1. The nuclei were stained with DAPI. The arrowheads indicate the recruitment of MGRN1 with mutant SOD1-positive aggregates. Scale bar, 20 μm. (E–F) COS-7 cells were transfected with a Myc-MGRN1 plasmid, and some cells were cotransfected with a FLAG-tagged SOD1G93A (F) construct. Transfected cells were treated with 15 μg/mL cycloheximide for 12 h, and some sets of cells were treated with 50 nM of Baf. The transfected-cell lysates were used for immunoblotting with anti-Myc, anti-SOD1, anti-FLAG, and anti-actin antibodies. (G–H) Quantification of the experimental data in Fig. 6E and F with NIH image analysis software represents the steady-state levels of wild-type SOD1 (G) and SOD1G93A (H) in the presence of overexpressed Myc-MGRN1 from three independent experiments. Represented values are presented as mean ± standard deviation of three independent experiments and $p < 0.05$ indicated the level of statistical significance for analyses.

MGRN1 overexpression accelerated the clearance of misfolded SOD1 inclusions partly through autophagy pathway and suppressed the intracellular aggregate formation of mutant SOD1.

3.5. MGRN1 confers cytoprotection against mutant SOD1 toxic species and improves cell viability

The synchronization of motor neuron pathology and abnormal protein accumulation in ALS has been previously explored (Ferraiuolo et al., 2011). However, the mechanism underlying the interplay of E3 ubiquitin ligases and the cytoprotection against proteotoxicity that is mediated by mutant SOD1 proteins in ALS largely remains unknown. Based on these intriguing observations, such as the diminished levels and aggregates of MGRN1 in motor neurons of SOD1-mutant mice and the preferential elimination of mutant SOD1 proteins by MGRN1 overexpression, we further investigated whether MGRN1 provided cytoprotection against the proteotoxicity of mutant SOD1 proteins. When the endogenous MGRN1 were depleted through small interfering RNA (siRNA), we observed the accumulation of mutant SOD1 proteins (Fig. 8A–D). In the cell viability assay, we noticed that the partial depletion of MGRN1 generated additive vulnerable effects in the cells expressing aberrant SOD1 proteins (Fig. 8E and F). To further validate this observation, we performed another set of cell viability assays in which we separately overexpressed MGRN1 or its catalytically inactive form $MGRN1^{AVVA}$ in SOD1G93A- (Fig. 8I) and SOD1G37R-expressing (Fig. 8J) cells with an Hsp70 chaperone construct. The cell viability analyses indicated that MGRN1 provided a defense against mutant SOD1 aggregation and that this effect was slightly more prominent in the cells coexpressing MGRN1 and Hsp70 chaperone. Overall, these results indicated that MGRN1 alleviated mutant SOD1-mediated cytotoxicity and possibly elicited a cascade of events, which included the functional recruitment of MGRN1 with multifactorial toxic inclusions of abnormal SOD1 proteins.

4. Discussion

Our present study shows that the MGRN1 E3 ubiquitin ligase interacted with both wild-type and mutant SOD1 proteins in cells. The overexpression of MGRN1 facilitated the degradation of mutant SOD1 proteins. Moreover, mutant SOD1 proteins dysregulated endogenous MGRN1 levels and overexpression of MGRN1 alleviated their proteotoxic insults. Taken together, the findings of all of these studies support our current conclusion that MGRN1 is a novel cytoprotective factor to alleviate mutant SOD1-mediated proteotoxicity.

Previous reports showed that mutations in MGRN1 cause spongiform neurodegeneration in mice (He et al., 2003). MGRN1-mutant mice also exhibit mitochondrial dysfunction at an early age (Sun et al., 2007). Subsequently, it has been observed that MGRN1 promotes monoubiquitination of tumor susceptibility gene 101 (TSG101). This observation elaborates a novel function of MGRN1 via proteasome-independent degradation pathway (Kim et al., 2007). Mutant MGRN1 causes spongiform neurodegeneration in mice and it also

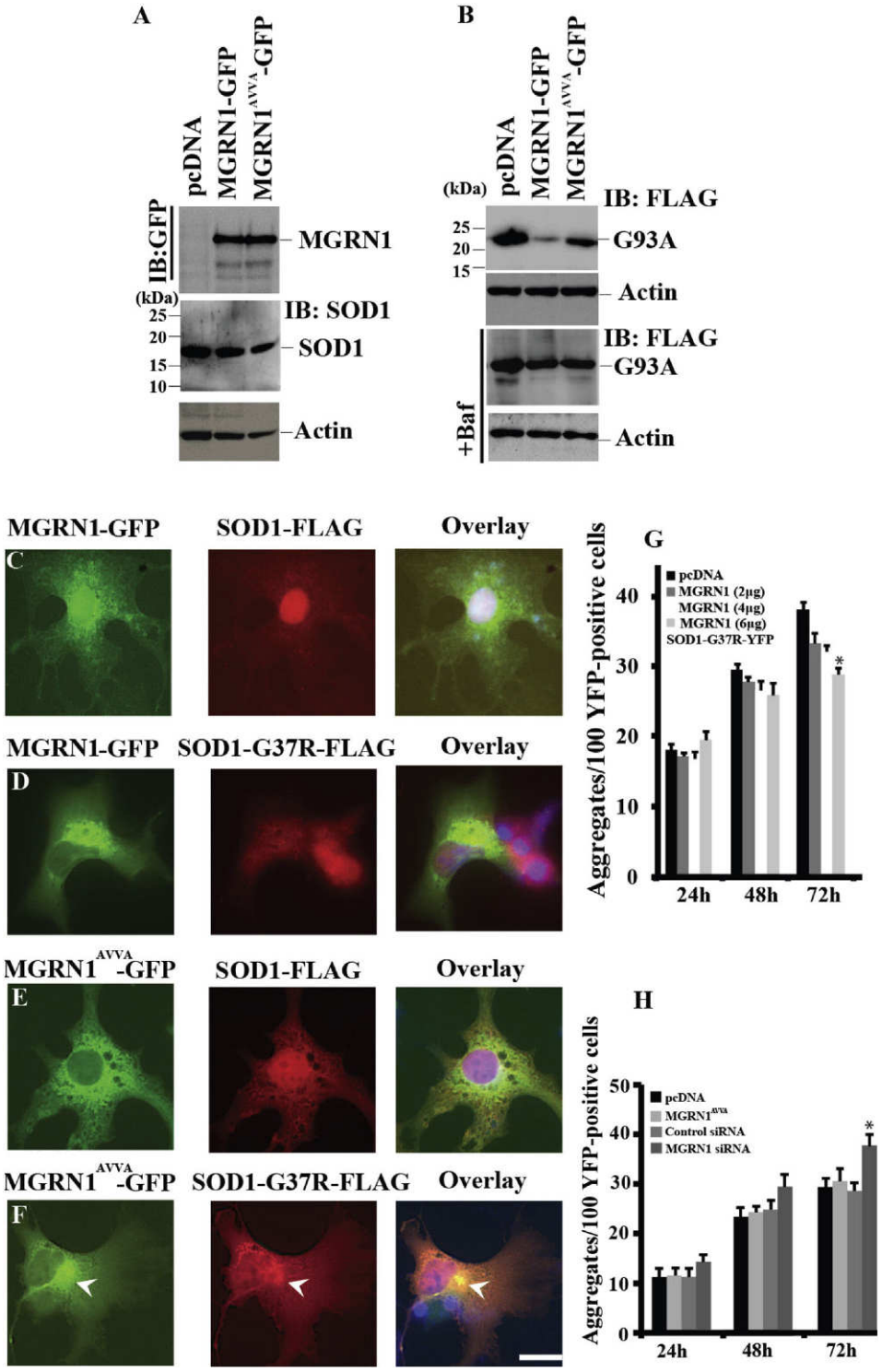

Fig. 7. MGRN1 suppresses mutant SOD1 aggregation in cells. (A) COS-7 cells were transfected with MGRN1-GFP or MGRN1^{AVVA}-GFP mutant constructs, and cell lysates were prepared after 48 h of transfection. All of the blots were sequentially developed with anti-GFP, anti-SOD1, and anti-actin antibodies. (B) COS-7 cells were cotransfected with MGRN1-GFP or MGRN1^{AVVA}-GFP in the presence of FLAG-tagged SOD1G93A, and some cells were treated with 50 nM of Bafilomycin (Baf) for 12 h prior to collection. Immunoblots were probed with anti-FLAG and anti-actin antibodies. (C–F) COS-7 cells were cotransfected with FLAG-tagged SOD1 (C, E) or FLAG-tagged SOD1G37R (D, F) plasmids with MGRN1-GFP (C, D) or MGRN1^{AVVA}-GFP mutant (E, F) plasmids, and, after 48 h, the cells were incubated with an anti-FLAG antibody. A rhodamine-conjugated secondary antibody was used to detect FLAG-tagged SOD1. DAPI was used to stain nuclei. Scale bar, 20 μm. (G–H) As described in sections C–F, some sets of YFP-tagged SOD1G37R-expressing COS-7 cells were cotransfected in a concentration-dependent manner with an empty vector (Control) and Myc-MGRN1 (G) or MGRN1 mutant, Scrambled siRNA and MGRN1-siRNA (H). The quantitative immunofluorescence analysis demonstrates SOD1G37R-YFP aggregates in 100 cells. The values are presented as the mean ± SD of three independent experiments and each performed in triplicate. *, $p < 0.05$ compared with (pcDNA or Scrambled siRNA) expressed cells.

interacts with cytosolic prion proteins (PrPs) (Chakrabarti and Hegde, 2009; He et al., 2003). Melanocortin receptors (MCRs) are also ubiquitinated as substrates of MGRN1 and are regulated by MGRN1 (Cooray et al., 2011). In contrast, our present study together with our recent works revealed a novel role of MGRN1 in recognizing misfolded proteins and in reducing proteotoxicity (Chhangani and Mishra, 2013; Chhangani et al., 2014b). In this work, mutant SOD1 proteins are identified as new target proteins recognized by MGRN1 in addition to mutant huntingtin and ataxin-3 proteins with expanded polyglutamine (Chhangani et al., 2014b). To date, several E3 ubiquitin-protein ligases, such as gp78 (Ying et al., 2009), MITOL (MARCH-V) (Yonashiro et al., 2009), Dorfin (Niwa et al., 2002), and E6-AP (Mishra et al., 2013), have been known to recognize and target misfolded SOD1 proteins for degradation through ubiquitin proteasome system (UPS). In comparison to those E3 ligases, MGRN1 is a unique E3 ligase catalyzing monoubiquitination, which eliminates misfolded proteins through UPS-independent pathway. Possibilities of MGRN1 to recognize other misfolded proteins linked to neurodegenerative diseases and the mechanisms of MGRN1-mediated protein degradation should be explored further.

We found that MGRN1 partially co-localizes with misfolded mutant SOD1 and preferentially degrades mutant SOD1. Moreover, degradation of mutant SOD1 is dependent on the activity of MGRN1 and is inhibited by bafilomycin, an inhibitor for autophagy. This is in line with our previous finding that inhibition of autophagy elevates the level of endogenous MGRN1 and recruits ubiquitin-positive aggregates in cells (Chhangani and Mishra, 2013). Together with the current findings that MGRN1 is partially recruited and colocalized with Lamp2 and p62, important components for autophagy-lysosomal pathway, MGRN1 facilitates degradation of misfolded protein through autophagy pathway. Since monoubiquitination of substrate protein determines its endocytosis and membrane trafficking (Polo et al., 2002), MGRN1 may participate in targeting mutant SOD1 to autophagy-lysosomal pathway. Moreover, association of MGRN1 with molecular chaperone, Hsp70 and preferential degradation of mutant protein by MGRN1 suggest that MGRN1 has a capability to target selectively aberrant proteins for their clearances with help of chaperones and components of autophagy-linked protein quality control mechanism (Chhangani and Mishra, 2013).

Previously, it has been observed that macroautophagy and the proteasome pathway alleviate mutant SOD1-mediated neurotoxicity (Kabuta et al., 2006). It has also been shown that macroautophagy promotes the degradation of mutant SOD1 proteins partly through the action of small heat shock protein HspB8, when aberrant SOD1 forms insoluble aggregates and impairs proteasomal activity (Crippa et al., 2010; Kabuta et al., 2006). Recently, we observed that administration of Cystatin C (CysC) provides cytoprotection against mutant SOD1-mediated toxicity partly through induction of autophagy (Watanabe et al., 2014). This study also support our hypothesis that MGRN1-mediated mutant SOD1 clearance via autophagy is effective, because

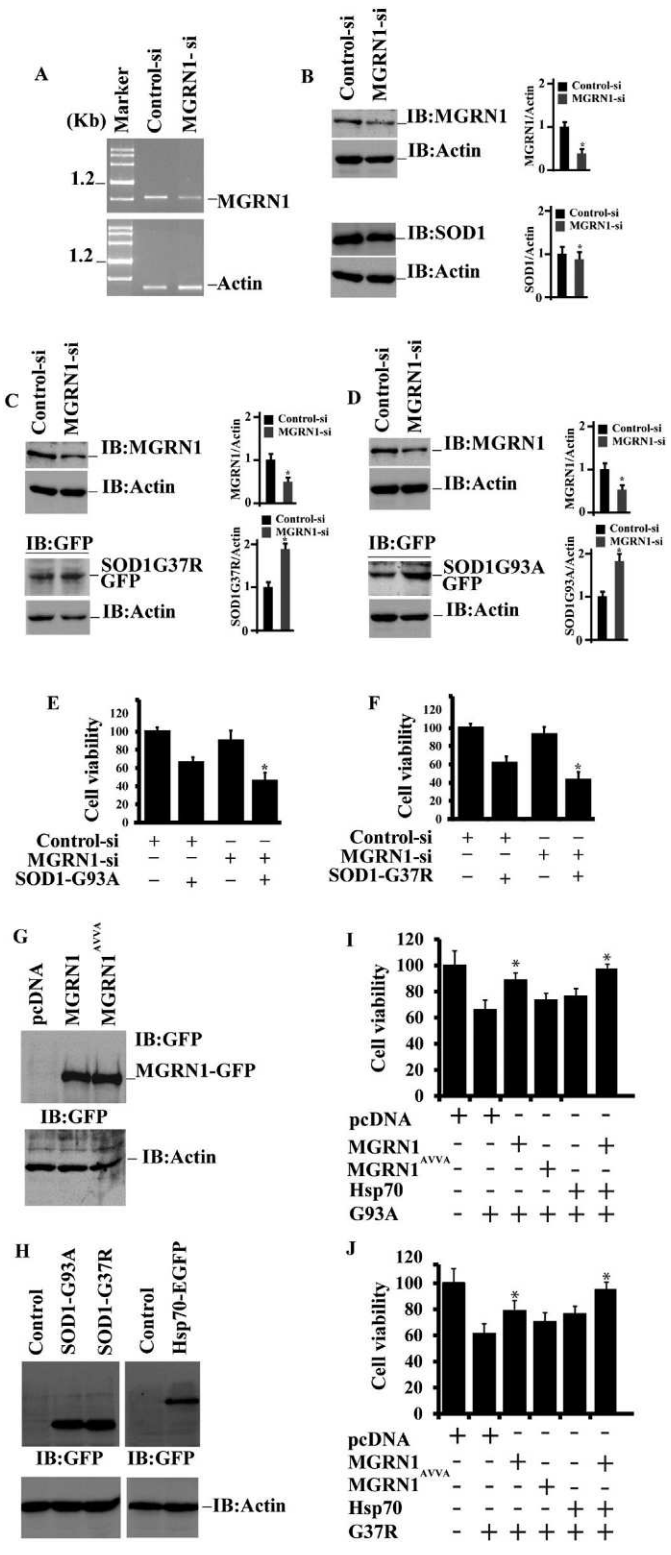

Fig. 8. MGRN1 alleviates the proteotoxicity generated by mutant SOD1 proteins and confers cytoprotection. (A–B) 293T cells were transfected with Control-siRNA or MGRN1-siRNA oligonucleotides. After 48 h of transfection of total RNA, cells were isolated and processed for reverse transcription-polymerase chain reaction analysis (A), and some sets of cells were used for immunoblotting (B) with anti-MGRN1, anti-SOD1, and anti-actin antibodies. (C–D) 293T cells were cotransfected with Control-siRNA or MGRN1-siRNA oligonucleotides and SOD1G37R (C) or SOD1G93A (D), and the blots were then probed with anti-MGRN1, anti-GFP, or anti-actin antibodies. (B–D, right) The levels of MGRN1 or SOD1 proteins relative to the ones of actin were plotted as mean ± SD. The blots were quantified from three different experiments with NIH Image analysis software. (E–F) 293T cells were transiently cotransfected with Control-siRNA or MGRN1-siRNA oligonucleotides and SOD1G93A (E) or SOD1G37R (F), as represented in the figure. Cells were harvested in 96-well tissue culture plates, and, after 72 h, cell viability was measured by a 3-(4,5-dimethylthiazol-2-yl)-2,5-diphenyltetrazolium bromide (MTT) assay. In bar graph, values are represented as mean ± SD of three independent experiments, performed in triplicate $^{*}p < 0.05$ compared to the mutant SOD1-expressing control siRNA-transfected cells as described in "Methods". (G-H) Immunoblot analysis of MGRN1-GFP or MGRN1^{AVVA}-GFP proteins (G) and mutant SOD1 and Hsp70-EGFP (H) in 293T cells transfected with the indicated expression plasmids used in (I, J). (I–J) As described in the previous section, the same set of cells was used for the cell viability analysis by a MTT assay of SOD1G93A- (I) and SOD1G37R- (J) transfected cells in the presence or absence of MGRN1, MGRN1^{AVVA}, or Hsp70 as indicated. The MTT assay was performed after 72 h of transfection. The values are presented as the mean ± SD. of three independent experiments, $^{*}p < 0.05$ compared to the mutant SOD1-expressing control cells and each experiment performed independently in triplicate.

UPS is known to be impaired in mutant SOD1 models. Through interaction with mutant SOD1 proteins, MGRN1 may facilitate their delivery into autophagosome or may improve efficient recognition of SOD1 by UPS through assisting the function of other E3 ubiquitin ligases by yet unidentified mechanism.

Our results suggested that MGRN1 overexpression dramatically suppressed the aggregation of mutant SOD1 proteins in cells and alleviated their associated cytotoxicity. A partial depletion of MGRN1 induced the cell death that is linked to mutant SOD1 proteins, and the diminished levels of MGRN1 in presymptomatic ALS mice contributed to the molecular mechanism of the disease. Taken together, our findings suggested MGRN1 is a novel cytoprotective factor to eliminate abnormal SOD1 through autophagy-lysosomal pathway. Considering that there are several known candidate cytoprotective factors against SOD1-mediated toxicities, the combination of these neuroprotective factors including MGRN1 may provide an opportunity for ameliorating the toxicities of mutant SOD1 and perhaps other misfolded proteins linked to neurodegenerative diseases.

Disclosure statement

The authors do not have any actual or potential conflicts of interests to disclose.

Acknowledgment

This work was supported by an Innovative Young Biotechnologist Award (IYBA) from the Department of Biotechnology Government of India (BT/06/IYBA/2012) (to A.M.); INSA-JSPS Joint Research Project Programme (IA/INSA-JSPS Project 2013-2016/4097) (to A.M. and K.Y.); Grants-in-Aid for Scientific Research (23111006) and Scientific Research (B) (26293208) from the Ministry for Education, Culture and Sports, Science and Technology, Japan; Grant-in-Aid for Research on rare and intractable diseases, the Research Committee on Establishment of Novel Treatments for Amyotrophic Lateral Sclerosis, from the Ministry of Health, Labour and Welfare of Japan; The Naito Foundation; and Uehara Memorial Foundation (to K.Y.). AM was also supported by a Ramalinganswami Fellowship, Government of India (BT/RLF/Reentry/11/2010). The authors would like to thank Mr. Bharat Pareek and Mr. Sachin Chinchwadkar for their technical assistance and the entire lab management during manuscript preparation. We would also like to thank the following for the generous gifts of plasmids: Dr. Wafik S. El-Deiry (Penn State Hershey Cancer Institute, Hershey, PA, USA) for the pcDNA3-cmyc, Dr. C. Olivares Sánchez and Dr. J.C. García-Borrón (University of Murcia, Murcia, Spain) for the pcDNA3-MGRN1 L (−)-myc plasmid, Dr. Teresa M. Gunn (McLaughlin Research Institute, Great Falls, MT, USA) for the MGRN1-GFP and MGRN1^{AVVA}-GFP constructs, Dr. Lois Greene (Laboratory of Cell Biology, NHLBI, NIH, Bethesda, MD, USA) for the pEGFP hsp70 construct, Dr. Douglas T Golenbock (University of Massachusetts Medical School, Worcester, MA, USA) for the pcDNA3-EGFP plasmid, and Elizabeth M. C. Fisher (Department of Neurodegenerative Disease, UCL Institute of Neurology, London, UK) for the GFP-SOD1^{G93A} and GFP-SOD1^{G37R}.

Appendix A. Supplementary data

Supplementary data to this article can be found online at http://dx.doi.org/10.1016/j.nbd.2015.11.017.

References

Allen, S., et al., 2003. Analysis of the cytosolic proteome in a cell culture model of familial amyotrophic lateral sclerosis reveals alterations to the proteasome, antioxidant defenses, and nitric oxide synthetic pathways. J. Biol. Chem. 278, 6371–6383.
Banerjee, R., et al., 2010. Autophagy in neurodegenerative disorders: pathogenic roles and therapeutic implications. Trends Neurosci. 33, 541–549.
Boillee, S., et al., 2006. Onset and progression in inherited ALS determined by motor neurons and microglia. Science 312, 1389–1392.
Bruijn, L.I., et al., 1997. ALS-linked SOD1 mutant G85R mediates damage to astrocytes and promotes rapidly progressive disease with SOD1-containing inclusions. Neuron 18, 327–338.
Bruijn, L.I., et al., 2004. Unraveling the mechanisms involved in motor neuron degeneration in ALS. Annu. Rev. Neurosci. 27, 723–749.
Chakrabarti, O., Hegde, R.S., 2009. Functional depletion of mahogunin by cytosolically exposed prion protein contributes to neurodegeneration. Cell 137, 1136–1147.
Cheroni, C., et al., 2009. Functional alterations of the ubiquitin-proteasome system in motor neurons of a mouse model of familial amyotrophic lateral sclerosis. Hum. Mol. Genet. 18, 82–96.
Chhangani, D., et al., 2013. Misfolded proteins recognition strategies of E3 ubiquitin ligases and neurodegenerative diseases. Mol. Neurobiol. 47, 302–312.
Chhangani, D., Mishra, A., 2013. Mahogunin ring finger-1 (MGRN1) suppresses chaperone-associated misfolded protein aggregation and toxicity. Sci. Rep. 3, 1972.
Chhangani, D., et al., 2014a. Autophagy coupling interplay: can improve cellular repair and aging? Mol. Neurobiol. 49, 1270–1281.
Chhangani, D., et al., 2014b. Mahogunin ring finger 1 suppresses misfolded polyglutamine aggregation and cytotoxicity. Biochim. Biophys. Acta 1842, 1472–1484.
Ciryam, P., et al., 2013. Widespread aggregation and neurodegenerative diseases are associated with supersaturated proteins. Cell Rep. 5, 781–790.
Cooray, S.N., et al., 2011. The E3 ubiquitin ligase Mahogunin ubiquitinates the melanocortin 2 receptor. Endocrinology 152, 4224–4231.
Crippa, V., et al., 2010. The small heat shock protein B8 (HspB8) promotes autophagic removal of misfolded proteins involved in amyotrophic lateral sclerosis (ALS). Hum. Mol. Genet. 19, 3440–3456.
Ferraiuolo, L., et al., 2011. Molecular pathways of motor neuron injury in amyotrophic lateral sclerosis. Nat. Rev. Neurol. 7, 616–630.
Gal, J., et al., 2009. Sequestosome 1/p62 links familial ALS mutant SOD1 to LC3 via an ubiquitin-independent mechanism. J. Neurochem. 111, 1062–1073.
Gunn, T.M., et al., 2013. MGRN1-dependent pigment-type switching requires its ubiquitination activity but not its interaction with TSG101 or NEDD4. Pigment Cell Melanoma Res. 26, 263–268.
Gurney, M.E., et al., 1994. Motor neuron degeneration in mice that express a human Cu,Zn superoxide dismutase mutation. Science 264, 1772–1775.
He, L., et al., 2003. Spongiform degeneration in mahoganoid mutant mice. Science 299, 710–712.
Hoffman, E.K., et al., 1996. Proteasome inhibition enhances the stability of mouse Cu/Zn superoxide dismutase with mutations linked to familial amyotrophic lateral sclerosis. J. Neurol. Sci. 139, 15–20.
Kabuta, T., et al., 2006. Degradation of amyotrophic lateral sclerosis-linked mutant Cu,Zn-superoxide dismutase proteins by macroautophagy and the proteasome. J. Biol. Chem. 281, 30524–30533.
Kikuchi, H., et al., 2006. Spinal cord endoplasmic reticulum stress associated with a microsomal accumulation of mutant superoxide dismutase-1 in an ALS model. Proc. Natl. Acad. Sci. U. S. A. 103, 6025–6030.
Kim, B.Y., et al., 2007. Spongiform neurodegeneration-associated E3 ligase Mahogunin ubiquitylates TSG101 and regulates endosomal trafficking. Mol. Biol. Cell 18, 1129–1142.
Li, L., et al., 2008. Altered macroautophagy in the spinal cord of SOD1 mutant mice. Autophagy 4, 290–293.
Lin, M.T., Beal, M.F., 2006. Mitochondrial dysfunction and oxidative stress in neurodegenerative diseases. Nature 443, 787–795.
Liu, J., et al., 2004. Toxicity of familial ALS-linked SOD1 mutants from selective recruitment to spinal mitochondria. Neuron 43, 5–17.
Mattiazzi, M., et al., 2002. Mutated human SOD1 causes dysfunction of oxidative phosphorylation in mitochondria of transgenic mice. J. Biol. Chem. 277, 29626–29633.
Mishra, A., et al., 2009. UBE3A/E6-AP regulates cell proliferation by promoting proteasomal degradation of p27. Neurobiol. Dis. 36, 26–34.
Mishra, A., et al., 2013. E6-AP association promotes SOD1 aggresomes degradation and suppresses toxicity. Neurobiol. Aging 34 (1310), e11–e23.
Mulherkar, S.A., et al., 2009. The ubiquitin ligase E6-AP promotes degradation of alpha-synuclein. J. Neurochem. 110, 1955–1964.
Niwa, J., et al., 2002. Dorfin ubiquitylates mutant SOD1 and prevents mutant SOD1-mediated neurotoxicity. J. Biol. Chem. 277, 36793–36798.
Perez-Oliva, A.B., et al., 2009. Mahogunin ring finger-1 (MGRN1) E3 ubiquitin ligase inhibits signaling from melanocortin receptor by competition with Galphas. J. Biol. Chem. 284, 31714–31725.
Polo, S., et al., 2002. A single motif responsible for ubiquitin recognition and monoubiquitination in endocytic proteins. Nature 416, 451–455.
Raoul, C., et al., 2002. Motoneuron death triggered by a specific pathway downstream of Fas. Potentiation by ALS-linked SOD1 mutations. Neuron 35, 1067–1083.
Srivastava, D., Chakrabarti, O., 2014. Mahogunin-mediated alpha-tubulin ubiquitination via noncanonical K6 linkage regulates microtubule stability and mitotic spindle orientation. Cell Death Dis. 5, e1064.
Sun, K., et al., 2007. Mitochondrial dysfunction precedes neurodegeneration in mahogunin (Mgrn1) mutant mice. Neurobiol. Aging 28, 1840–1852.
Upadhyay, A., et al., 2015. Mahogunin ring finger-1 (MGRN1), a multifaceted ubiquitin ligase: recent unraveling of neurobiological mechanisms. Mol. Neurobiol. http://dx.doi.org/10.1007/s12035-015-9379-8.
Urushitani, M., et al., 2002. Proteasomal inhibition by misfolded mutant superoxide dismutase 1 induces selective motor neuron death in familial amyotrophic lateral sclerosis. J. Neurochem. 83, 1030–1042.
Vijayvergiya, C., et al., 2005. Mutant superoxide dismutase 1 forms aggregates in the brain mitochondrial matrix of amyotrophic lateral sclerosis mice. J. Neurosci. 25, 2463–2470.

Wanker, E.E., et al., 1999. Membrane filter assay for detection of amyloid-like polyglutamine-containing protein aggregates. Methods Enzymol. 309, 375–386.
Watanabe, M., et al., 2001. Histological evidence of protein aggregation in mutant SOD1 transgenic mice and in amyotrophic lateral sclerosis neural tissues. Neurobiol. Dis. 8, 933–941.
Watanabe, S., et al., 2014. Cystatin C protects neuronal cells against mutant copper-zinc superoxide dismutase-mediated toxicity. Cell Death Dis. 5, e1497.
Wong, E., Cuervo, A.M., 2010. Autophagy gone awry in neurodegenerative diseases. Nat. Neurosci. 13, 805–811.
Wong, P.C., et al., 1995. An adverse property of a familial ALS-linked SOD1 mutation causes motor neuron disease characterized by vacuolar degeneration of mitochondria. Neuron 14, 1105–1116.
Yamanaka, K., et al., 2008. Astrocytes as determinants of disease progression in inherited amyotrophic lateral sclerosis. Nat. Neurosci. 11, 251–253.
Ying, Z., et al., 2009. Gp78, an ER associated E3, promotes SOD1 and ataxin-3 degradation. Hum. Mol. Genet. 18, 4268–4281.
Yonashiro, R., et al., 2009. Mitochondrial ubiquitin ligase MITOL ubiquitinates mutant SOD1 and attenuates mutant SOD1-induced reactive oxygen species generation. Mol. Biol. Cell 20, 4524–4530.
Zhang, F., et al., 2007. Interaction between familial amyotrophic lateral sclerosis (ALS)-linked SOD1 mutants and the dynein complex. J. Biol. Chem. 282, 16691–16699.